

Insights into Genetic and Proteomic Landscape of Pediatric Acute Lymphoblastic Leukemia

ABSTRACT

Background. Despite excellent survival, relapse occurs in 20% of children with ALL. Deep analyses of cell signaling pathways allow us to identify new markers and/or targets promising a higher efficacy and less toxicity therapy. We investigated the expression of *CK2*, *MYC* and *ERG* in specific subgroups of pediatric ALL (B- and T-lineage) and the PI3K/Akt/mTOR (PI3K) signaling pathway in T-cell acute lymphoblastic leukemias.

Methods. We analyzed 61 diagnostic samples collected from 35 patients with B- and 26 with T-ALL, respectively. We evaluated expression of *CK2*, *MYC* and *ERG* genes using Sybr-Green assay and the comparative $2^{-\Delta\Delta C_t}$ method using 20 Healthy Donors (HDs). Moreover, we determined the expression of PI3K and JAK-STAT signaling components in both primary and immortalized T-ALL cells as well as in normal T cells using an optimized cytometric method for accurate proteomic profiling of T-ALL leukemic blasts at single-cell level.

Results. We observed a statistically significant difference in *CK2* expression in non-HR (p=0.010) and in HR (p=0.0003) T-ALL cases compared to HDs. T-ALLs with *PTEN*-Exon7 mutation, *IKZF1* and *CDKN2A* deletions showed a high *CK2* expression. *MYC* expression was higher in pediatric T-ALLs than HDs (p=0.019). Surprisingly, we found a *MYC* expression higher in non-HR than in HR T-ALLs. *TLX3* (*HOX11L2*) rearranged T-ALLs (27%) in association with *CRLF2* overexpression (23%) showed a very high *MYC* expression. In B-ALLs, we detected a *CK2* expression higher than HDs and *MYC* overexpression in HR compared to non-HR, particularly in *MLL*-rearranged B-ALLs. We observed a strong difference of *ERG* expression between pediatric T- and B-ALL cases.

About proteomic profile of T-ALLs, we observed that PTEN Exon 7 mutated T-ALL cells retain a distinct PI3K activation in particular these cells show higher pAkt levels and a lower pS6 expression. Interestingly we demonstrated for the first time that PTEN Exon 7 mutated T-ALL are non-responsive to IL7 in vitro as assessed by lack of pSTAT5 activation, although they do express IL7R.

Conclusions. We confirmed *CK2* as a prognostic marker and a therapeutic target. In pediatric B-ALLs, high expression of *MYC* is related to HR features. We also observed an opposite impact of *ERG* expression in T- rather than B-ALLs. About phospho-proteomic data, we show as Phosphoflow analysis represents a fast, reliable and accurate method to study the signaling profile of T-ALL. PTEN Exon7 mutated T-ALL cells are not responsive to IL7 in vitro suggesting that they may activate other mechanisms to support their viability and proliferation such as a higher constitutive PI3K/Akt signaling. Our observations should be considered in future studies aiming at molecular targeting of PI3K and/or JAK/STAT pathways for pharmacological intervention in T-ALL.

Keywords

Acute Lymphoblastic Leukemia, childhood, CK2, MYC, ERG, Phosho-flow, PTEN, JAK/STAT, Interleukin 7, Cell signaling

INTRODUCTION

Substantial advances have been made in the past five decades in the treatment of patients with acute lymphoblastic leukemia (ALL), the most common malignancy in childhood. In contemporary ALL treatment regimens, patients are stratified into different risk groups based on clinical and biologic characteristics at presentation as well as on early treatment response. Improved understanding of the biologic heterogeneity of ALL and the development of sensitive polymerase chain reaction-based or flow cytometry-based minimal residual disease (MRD) response-monitoring techniques have facilitated modern risk stratification for childhood ALL [1]. Despite excellent survival for most pediatric patients with ALL, relapse occurs in 15% to 20% of children and remains the first cause of death in children with cancer [2]. Approximately 75% of patients with B-lineage ALL have somatic aneuploidy or recurrent chromosomal translocations, many of which have prognostic significance [3]. Conversely, the clinical significance of most recurrent genomic alterations in T-lineage ALL is less clear, and current clinical trials stratify patients with T-ALL, based on response to 8-days of prednisone administration or detection of MRD during induction phase [4,5]. Moreover, early relapses of both B- and T-ALL are a current challenge because the high rate of second line treatment failure. For this reason, analyses of significantly enriched signaling pathways might help to identify new markers and/or targets for tailored therapy. Pathways including WNT/ β -Catenin, p53 and PI3K/AKT/PTEN with ERG overexpression may contribute to the dysregulation of kinase signaling such as Casein Kinase 2 (CK2), which results in resistance to kinase inhibitors [6,7]. PI3K/Akt is a major signaling pathway implicated in T-ALL malignant transformation promoting several functions including cell survival and proliferation [8]. The major negative regulator of this pathway is the tumor suppressor lipid phosphatase and tensin homolog (PTEN), a lipid phosphatase that dephosphorylates PIP3 into PIP2, which is frequently inactivated in human cancer [9,10]. Constitutive hyperactivation of the PI3K/Akt pathway is a very common event in T-ALL that is

involved in sustaining leukemic cell viability and maintenance, and there is evidence that it can be aberrantly activated by cell-autonomous lesions [11-13]. PTEN non-sense or frame-shift mutations cluster in exon 7, resulting in a C-terminal truncated protein, rapidly degraded and thus leading to a decreased or absent PTEN protein expression and activity [14-16], however the prognostic significance of PTEN inactivation and PI3K/AKT aberrant activation is still unclear [17-19]. PTEN mutations, resulting in loss of PTEN protein, were reported in 17% of T-ALLs [20]. Furthermore, more than 85% of T-ALLs have been shown to display hyperactivated signaling due to post-translational inactivation of PTEN by casein kinase 2 (CK2)-mediated phosphorylation and/or oxidation by reactive oxygen species (ROS) [16,21]. The majority of PTEN alterations occur at the level of exon 7, and are caused by small insertion/deletions that lead to truncation of the protein due to premature termination of translation [16,22].

Interleukin 7 (IL7) promotes cell survival and cell cycle progression during normal T-cell development [23,24]. Upon ligand binding, the IL7 receptor (IL7R) dimerizes and induces the phosphorylation of JAK3 and JAK1 [25]. Activated JAKs allow the recruitment and phosphorylation of signal transducer and activator of transcription 5 (STAT5), which in turn can regulate the transcription of target genes such as B-cell CLL/lymphoma2 (BCL-2) family members [26]. It has been recently demonstrated that IL7 mediated upregulation of Bcl-2 in T-ALL is independent of STAT5 activity, suggesting that STAT5 could promote the viability of malignant T cells by alternative Bcl-2 independent mechanisms. Moreover, it has been showed that STAT5 directly downregulates BCL6 and promotes the expression of PIM1 in response to IL7 stimulation [27].

IL7/IL7R pathway can promote leukemogenesis *in vivo* [28,29], or can drive disease progression by regulating cell viability and proliferation [25,30].

Barata J and Melao A showed for the first time that IL7 activity crosstalks with Casein Kinase 2 (CK2)-mediated signaling in T-ALL cases [31]. CK2 is a key regulator in PI3K/AKT pathway. An

important *CK2* target is Ikaros (*IKZF1*), a transcription factor that displays crucial functions in the hematopoietic system and controls the development mainly in early B- and T-cells. Mutations that lead to reduced Ikaros function or expression have also been found to be a major genetic feature in human B-cell acute lymphoblastic leukemia (B-ALL) [32] and loss of Ikaros also promotes the development of T-cell lymphoma/leukemia in mice, which suggests that Ikaros acts as a tumor suppressor in T-cell acute lymphoblastic leukemia (T-ALL) and B-ALL. However, evidence linking Ikaros to human T-ALL has been sometimes contradictory and elusive. Despite the low prevalence, Ikaros loss of function is clearly a recurrent anomaly in human T-ALL. Thus, Ikaros inactivation could play a causal role in disease progression in a subset of T-ALL cases. [33]. Another proto-oncogene closely involved in many cancers, including leukemia, is *MYC*. Aberrant expression of *MYC* in leukemia results in an uncontrolled rate of proliferation and, thereby, a blockade of the differentiation process. *MYC* is not activated by mutations in the coding sequence, but its overexpression in leukemia is mainly caused by gene amplification and aberrant regulation of its transcription [34]. A tightly controlled increase in *MYC* expression is required for differentiation, but prolonged and excessive *MYC* activity is oncogenic and leads to increased proliferation, altered adhesion and chromatin remodeling [35]. Synergistic interactions between *CK2* and *MYC* might be due to a functional interaction of the two molecules that lead to lymphocyte transformation [36]. *CK2* inhibitors act as an Ikaros activator and suppress c-*MYC* in an Ikaros-dependent manner in the ALL cells. Recent data also indicated that in adult ALL patients, high c-*MYC* expression correlates with clinical high-risk factors and high proliferation markers. Several genes are involved in hematopoiesis control and therefore their deregulation can lead to hematological malignancies including leukemia. Another useful marker in paediatric leukemia is the Ets-related gene *ERG* (erythroblastosis virus E26 transforming sequence family member) that has an important role in early hematopoiesis and hematopoietic stem cell (HSC) maintenance [7]. *ERG* is preferentially and strongly expressed in the immature B- and T-lymphoid lineages, in addition to myeloid lineage

cells. Previous studies suggest that *ERG* overexpression is associated with inferior clinical outcome [37]. In T-ALL patients, a high level of *ERG* expression has been associated with poor relapse-free survival [38]. Zhao et al. demonstrated that in childhood B-ALL patients, *ERG* was not an independent prognostic factor, for either OS or for RFS. Furthermore, in childhood B-ALL low *ERG* expression was associated with higher WBC counts, higher relapse rate and poor RFS [39]. The expression of *CK2* in association with *MYC* and *ERG* has not been characterized in biological subgroups of pediatric ALL, yet. The characterization of these genes in a cohort of pediatric B- and T-ALL, would integrate new markers of disease and/or therapeutic targets in ALL.

About phospho-proteomic signaling, although Western Blotting (WB) is the gold standard technique to study the proteomic profile of hematological malignancies, phosphoflow cytometry has been shown to provide several advantages over WB such as real time measurement of multiple and simultaneous events in single cells [40], as well as the characterization of rare subsets of cells even within heterogeneous samples [41].

In this study, we have characterized PI3K/Akt/mTOR (PI3K) and JAK-STAT pathways at single cell level within a cohort of pediatric T-ALL patients by carrying out phosphoflow cytometry. The results reported herein show that PTEN exon 7 mutated T-ALL display a distinct signaling pathway and that phosphoflow approach is a feasible and robust tool for accurate investigation of this subset of T-ALL patients including in vitro screening of targeted inhibition molecules.

MATERIALS AND METHODS

Primary Patient samples

We included in our “molecular characterization” 26 patients with T-ALL and 35 with B-ALL diagnosed in Center of Pediatric Hematology Oncology, Azienda Policlinico /San Marco of Catania from 2000 to 2016. The last one cohort (B-ALL) included the following biological subgroups: 8 with t(9;22) or Ph+, 16 with t(12;21); 4 with 11q23 rearranged (-R) and 7 without known translocations defined as “B-others”, respectively. Based on protocol response stratification criteria, patients were classified as Standard Risk (SR) e Intermediate Risk (MR) or non-HR (n=17) and High Risk (n=18) in B-ALL, while as HR (n=11) and non-HR (n=15) for T-ALL patients, respectively. Patients received treatment according to the ongoing protocols [AIEOP-BFM ALL2000/R2006 and ALL2009, respectively]. We routinely study biopsy material of leukemia patients at diagnosis by performing morphologic, immune-phenotype, cytogenetic and molecular biology analyses. The expression levels of *CK2*, *MYC* and *ERG* genes were retrospectively analyzed in cDNA collected from 61 diagnostic samples of children with ALL (median age 7 years; range 1-18 years; 32 males and 29 females). Biological and clinical features are shown in **Table 1**. As “proteomic characterization” Bone marrow (BM) or peripheral blood (PB)-derived leukemic cells were collected from 25 children with T-ALL enrolled in the AIEOP ALL 2009 or R2006 protocols at the Pediatric Clinic of University Milano Bicocca, at San Gerardo Hospital. Mononuclear cells were collected by Ficoll-Paque centrifugation, washed twice in culture medium (RPMI-1640 supplemented with 10% FBS) and then cryopreserved in RPMI-1640 with 10% DMSO. All specimens consisted of 85%-100% of blasts. Features of these patients are summarized

in **S-Table1**. Moreover, we collected 11 BM control samples from patients without hematological diseases.

An institutional review board approval and an informed consent from parents were obtained, according to our hospital regulations.

Table 1. Biological and clinical features of 61 children with ALL analyzed for expression of CK2-MYC-ERG

	T-ALL n=26 n(%)	B-ALL n=35 n(%)	Total n=61 n(%)
<i>Gender</i>			
Female	6 (23)	22 (63)	28 (46)
Male	20 (77)	13 (37)	33 (54)
<i>Age at diagnosis (years)</i>			
1-9	10 (38)	27 (77)	37 (61)
≥10	16 (62)	8 (23)	24 (39)
<i>Presenting WBC count/μl</i>			
<10.000	4 (16)	12 (34)	16 (26)
10.000-50.000	3 (11)	11 (32)	14 (23)
50.000-100.000	8 (31)	2 (6)	10 (16)
≥100.000	11 (42)	10 (28)	21 (35)
<i>Prednisone response[^]</i>			
Good	17 (65)	27 (77)	44 (72)
Poor	9 (35)	8 (23)	17 (28)
<i>MRD risk group*</i>			
Standard risk	3 (12)	9 (26)	12 (20)
Intermediate risk	14 (54)	19 (54)	33 (54)
High risk	4 (15)	7 (20)	11 (18)
Not performed	5 (19)	-	5 (8)
<i>Final risk group§</i>			
SR+MR (non-HR)	15 (58)	16 (46)	30 (49)
HR	11 (42)	19 (54)	31 (51)
<i>Event</i>			
No	18 (69)	24 (69)	42 (69)
Yes	8 (31)	11 (31)	19 (31)
<i>Outcome</i>			
Alive	19 (73)	28 (80)	47 (77)
DOC	5 (19)	4 (11)	9 (15)
DOD	2 (8)	3 (9)	5 (8)

Table 1 Legend: ^Good: <1000 leukemic blasts/ μ l after 7 days of Prednisone administration; Poor \geq 1000/ μ l. *Minimal Residual Disease (MRD) Standard risk: negative both at day +33 (end of induction or phase Ia) and day +78 (end of consolidation therapy of Phase Ib); High risk: MRD level \geq 10⁻³ at day +78; Intermediate risk: all others (AIEOP-BFM ALL 2000-2009).

§ Patients with a BCR-ABL or MLL/KMT2A rearrangement positivity at diagnosis or a prednisone poor-response (PPR) or \geq 10% blasts (detected by cytofluorimetry) at day+15 BM (for those who were enrolled at AIEOP-BFM-ALL 2009 protocol) or induction failure (\geq 5% blasts at day+33 BM), were stratified into the HR final group independently from MRD results. Events were considered: relapse or death of disease (DOD) or death of complication (DOC) during treatment.

Supplementary Table 1: Biological and clinical features of 25 T-ALL patients

Patients ID	Sex	Age (Years)	WBC/mm ³ at diagnosis	Blasts at diagnosis in BM/PB (%)	Prednisone Response	Immunophenotype (EGIL Classification)	<i>PTEN</i> Status	<i>IL7Rα</i> (Exon6)	<i>CRLF2</i> (Exon6)	<i>STAT5B</i> (Exon16)	<i>TAL1</i> status	<i>ETP</i> status
UPN#1	M	13	84300	98	PGR	T-IV	mut	wt	wt	wt	wt	no
UPN#2	F	13	1026000	98	PPR	T-IV	mut	SNP	wt	wt	mut	no
UPN#3	F	13	400000	98	PGR	T-III	mut	wt	wt	wt	wt	no
UPN#4	M	15	169570	90	PPR	TI/II	mut	wt	wt	wt	wt	no
UPN#5	F	10	136720	95	PGR	T-III	mut	wt	wt	wt	wt	no
UPN#6	M	14	88900	98	PGR	T-IV	wt	wt	wt	wt	wt	no
UPN#7	M	6	60050	90	PGR	T-III	wt	wt	SNP	wt	wt	no
UPN#8	F	3	130300	95	PPR	T-III	wt	SNP	wt	wt	wt	no
UPN#9	M	8	74060	98	PGR	T-III/IV	wt	wt	wt	wt	wt	no
UPN#10	M	13	110310	90	PPR	TI/II*	wt	nv	nv	nv	wt	yes
UPN#11	M	2	4050	95	PGR	T-III	wt	wt	wt	wt	wt	no
UPN#12	M	9	5900	45	PGR	TI/II*	wt	SNP	wt	wt	wt	yes
UPN#13	M	9	14630	90	PGR	T-III	wt	SNP	SNP	wt	wt	no
UPN#14	M	7	6820	28	PGR	TI/II	wt	SNP	wt	wt	wt	no
UPN#15	M	12	9390	70	PGR	T-III	wt	SNP	wt	wt	wt	no
UPN#16	F	6	14350	90	PGR	T-III	wt	SNP	wt	wt	wt	no
UPN#17	M	11	159580	76	PPR	TI/II	wt	nv	nv	nv	wt	no
UPN#18	F	2	103700	60	PPR	T-IV	wt	SNP	wt	wt	wt	no
UPN#19	M	3	369810	90	N.A.	T-III	mut	wt	wt	wt	wt	no
UPN#20	M	14	168090	90	PPR	T-IV	mut	wt	wt	wt	wt	no
UPN#21	F	5	362800	90	N.A.	T-III	wt	wt	wt	wt	wt	no
UPN#22	M	6	14420	95	PGR	T-III	wt	wt	wt	wt	wt	no
UPN#23	M	17	15800	80	PGR	T-III	wt	wt	SNP	wt	wt	no
UPN#24	F	6	6300	90	PGR	T-III	wt	mut	SNP	wt	wt	no
UPN#25	M	16	15220	95	PGR	T-IV	wt	wt	wt	wt	wt	yes

PPR= Prednisone Poor Responder

PGR= Prednisone Good Responder

ETP= Early T cell Precursor according to Coustan-Smith et al.

mut=mutated

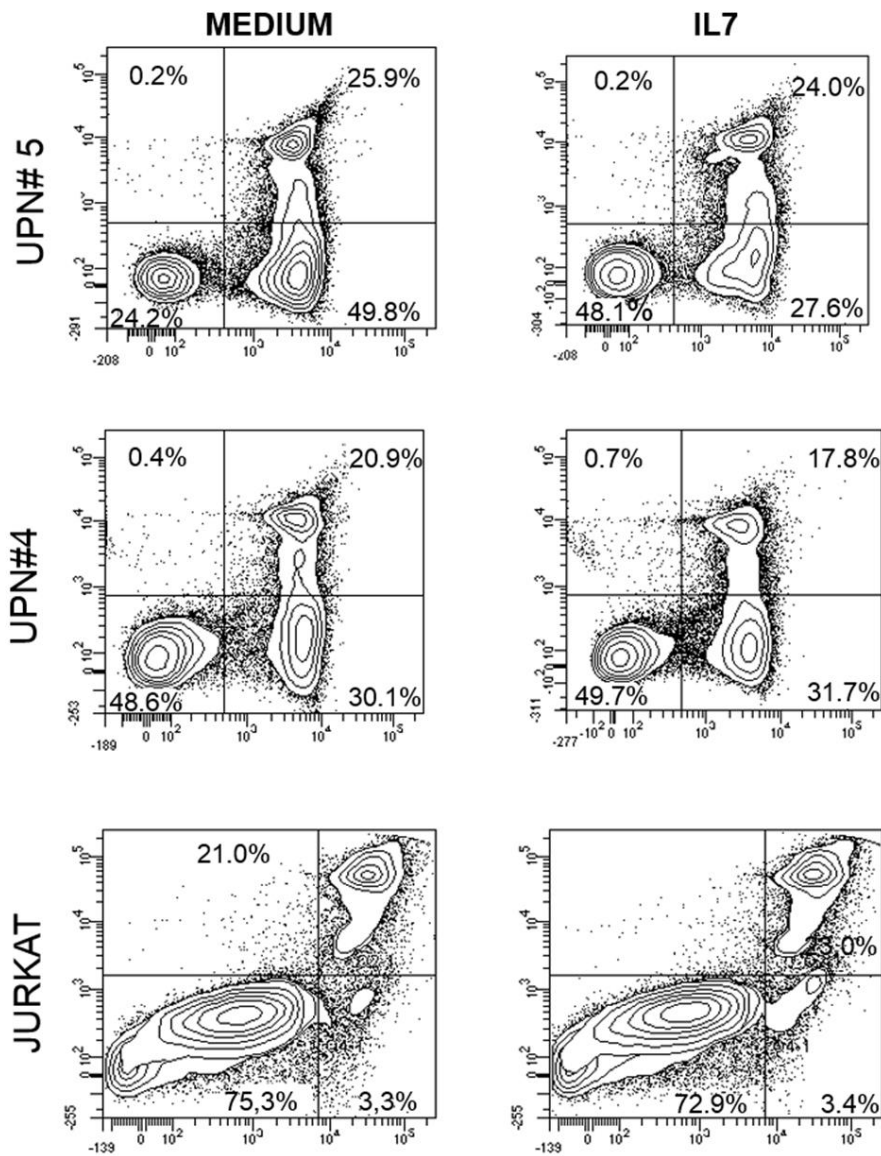
wt=wild type

Cell lines cultures and human normal bone marrows

CCRF-CEM (T-ALL bearing *PTEN* and *CDKN2A* deletions) and JURKAT (T-ALL bearing *PTEN* missense mutation, *CDKN2A* and *CREBBP* deletion) cell lines were used as T-ALL positive controls. REH (B-ALL bearing *ETV6/RUNX1* translocation) and MHH-CALL-4 (B-ALL bearing *JAK2-I682F* mutation, constitutive phosphorylation of *JAK2* and *STAT5* and *CRLF2* overexpression) were used as B-ALL positive controls (ATCC) (**Supplementary Materials**).

Twenty samples of bone marrow (BM) from children without a history of malignancy (healthy donors for bone marrow transplantation) were selected and served as healthy donors (HDs). We collected an informed consent from their parents, before bone marrow donation. In addition, Thymocytes were also analyzed as normal internal control about *CK2*, *MYC* and *ERG* expression respect to Healthy Donors (**Supplementary Materials**).

CEM, Jurkat and HPB-ALL T-ALL cell lines were also used about proteomic study and were cultured in RPMI-1640 medium supplemented with 10-20% fetal bovine serum (FBS), 100 IU/ml penicillin, 100 µg/ml streptomycin and 1% L-glutamine, at 37°C in humidified air containing 5% CO₂. 293T cell line (cultured in DMEM high glucose with 10% FBS) and CEM were used respectively as positive and negative control for *PTEN* comparative detection in WB and phosphoflow analysis. Cell survival experiments with either primary T-ALL samples or Jurkat cells are briefly described: cells were cultured in RPMI-1640 medium supplemented with 5% FBS and 25 ng/ml of recombinant human IL7 (Peprotech) and cell viability was determined at 72 hours using annexin V-7AAD apoptosis kit and the manufacturer's instructions (R&D System) (**Supplementary Figure 1**).



Annexin V

Supplementary Figure 1. Thawed primary T-ALL samples were checked for count and viability with trypan blue dye. Average $0.5 \times 10^6/\text{ml}$ cells were cultured in triplicates in 24-well plates in medium alone or with IL7 (50 ng/mL) for 72 hours before harvest. Viability was determined using annexin V-based apoptosis detection kit. In the Figure above, we report the cytometric analysis in of 2 primary T-ALL samples (both *PTEN* exon 7 mutated) and in Jurkat cells.

RNA isolation and RT-qPCR

Mononuclear cells from BM samples were isolated by Ficoll gradient centrifugation and cryopreserved. Total RNA was extracted using TRizol Reagent (Invitrogen, CA, USA) following the manufacturer's protocols. First strand cDNA was synthesized from total RNA with reverse transcriptase and random primers, using the Superscript Reverse Transcriptase (Invitrogen, CA, USA). Samples were selected based on the quality and quantity of RNA (OD₂₆₀/OD₂₈₀ ratio: 1.8-2.0). Quantitative Real-Time RQ-PCR was performed with a 96-well optic plate using the QuantStudio 7 Flex (Applied Biosystem, Life Technologies). Each sample was tested in duplicate. Expression levels were normalized by *GUS* (endogenous control) and calculated by using the comparative $2^{-\Delta\Delta C_t}$ method. The Comparative Cycle Threshold (CCT) method was used to determine the relative expression levels of *CK2*, *MYC* and *ERG*, using the median of ΔC_t from HDs in two replicates and expressed as $2^{-\Delta\Delta C_t}$ ($\Delta C_t = GUS - \text{gene of interest}$). Primers' sequence of *CK2*, *MYC*, *ERG* and *GUS* and PCR protocols are shown in **Supplementary Materials**.

In addition, T-ALL patients were screened for the following molecular alterations: *PTEN-Exon7* mutations; *CALM-AF10* fusion transcript; *TP53* and *pS6* mutations; *TXL3* rearrangements and *CRLF2* overexpression, respectively.

Molecular Data Analysis

Patients were classified as having *high* or *low* *CK2* or *MYC* or *ERG* expression. We used as cut-off the median value of gene expression fold changes. Statistical analysis was performed using the GraphPad Prism 7 Software. The data are presented as the Mean \pm Standard Deviations (SDs). A two-tailed $P < 0.05$ was indicative of a statistically significant difference between groups (**Supplementary Materials**).

Flow cytometry immunophenotyping

Immunophenotyping at diagnosis was performed by standard multiparametric flow cytometry (FC) on fresh samples processed within 24 hours from collection. The diagnosis of T-ALL was based on standard criteria. Briefly, whole blood nucleated cells were incubated with a cocktail of conjugated monoclonal antibodies (MoAbs) for 15 minutes at room temperature and 30,000 total events for each tube were acquired on a FACScanto II™ flow cytometer (Becton Dickinson) and analyzed with Diva™ software (Becton Dickinson). A summary of the diagnostic immunophenotyping performed in the studied patients is reported in **S-Table 2**.

Supplementary Table 2 Immunophenotype of 25 T-ALL patients

Patients ID	Immunophenotyping											
	HLA-DR	CD34	smCD3	cyCD3	CD7	CD4	CD8	CD13	CD33	CD1a	CD2	CD5
UPN#1	-	+	+	+	+	+	+	-	+	-	+	<i>not tested</i>
UPN#2	-	+	+	+	+	+	+	-	-	-	+	+
UPN#3	-	-	+	+	+	+	+	-	-	+	+	+
UPN#4	-	+	+	+	+	-	+	+	-	-	+	+
UPN#5	-	-	+	+	+	+	+	+	-	+	+	+
UPN#6	-	-	+	+	+	+	+	-	-	-	+	+
UPN#7	-	-	+	+	+	+	+	-	-	+	-	+
UPN#8	-	-	+	+	+	+	+	-	-	+	+	+
UPN#9	-	-	+	+	+	+	+	-	-	+	+	+
UPN#10*	-	+	-	+	+	-	-	-	+	-	-	<i>not tested</i>
UPN#11	-	-	+	+	+	+	+	-	-	+	+	+
UPN#12*	+	+	-	+	+	-	-	-	-	-	+	+
UPN#13	-	-	+	+	+	+	+	-	-	+	+	+
UPN#14	-	+	+	+	+	+	-	+	-	-	+	+
UPN#15	-	-	-	+	+	+	-	-	+	-	+	+
UPN#16	-	-	+	+	+	+	+	+	-	+	+	+
UPN#17	-	-	-	+	+	+	-	+	+	-	+	+
UPN#18	-	+	+	+	+	+	-	-	-	-	-	+
UPN#19	-	+	+	+	+	+	-	-	-	+	+	+
UPN#20	-	+	+	+	+	+	-	-	-	-	+	+
UPN#21	-	+	+	+	+	+	+	-	-	+	+	+
UPN#22	-	-	+	+	+	+	+	-	-	+	+	+
UPN#23	-	-	+	+	+	+	+	-	-	+	+	+
UPN#24	-	-	-	+	+	+	-	-	-	+	-	+
UPN#25*	-	+	+	+	+	-	-	+	+	-	+	-

*ETP

Phosphoflow cytometry

Thawed mononuclear cells from primary T-ALL samples were assessed for count and viability with trypan blue die before phosphoflow testing. Fresh cell lines or primary thawed cells were starved in X-VIVO medium and rested at 37°C for 16 hours or 1 hour respectively, thereafter cells viability was checked again, and only samples with $\geq 70\%$ of viability were used for phosphoflow experiments. Then cells were stimulated with IL7 [50 ng/mL] or inhibited with NVP-BEZ 235 [800 nM] and incubate 15 or 30 minutes at 37°C respectively. Cells were then fixed with 1.5% paraformaldehyde and permeabilized with 90% ice-cold methanol (prior to staining with anti-phospho-protein-directed MoAbs (or isotype matched IgG) and surface antigen-directed MoAbs anti-CD7 ECD (Beckman Coulter) and anti CD45 PerCP (BD). Characteristics of MoAbs are described in **S-Table 3**.

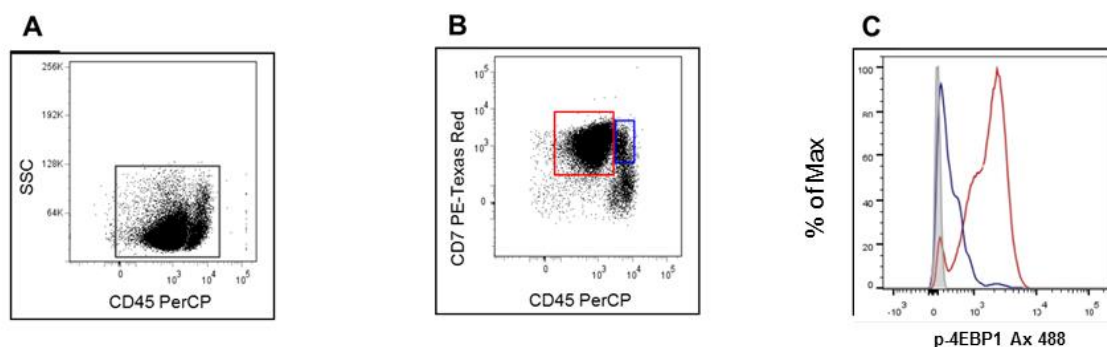
Supplementary Table 3 Characteristics of selected antibodies and staining combinations for phosphoflow assay

Selected Antibodies				
Reactivity	Clone	Fluorochrome	Source	Ig class
IgG1 k Isotype control	DA1E	Alexa Fluor 488	Cell Signaling	Rabbit IgG
IgG1 Isotype control	DA1E	Alexa Fluor 647	Cell Signaling	Rabbit IgG
IgG1 Isotype control	MOPC-21	Alexa Fluor 488	BD	Mouse IgG ₁ k
IgG1 Isotype control	MOPC-21	PE (Phycoerythrin)	BD	Mouse IgG ₁ k
IgG1 Isotype control	MOPC-21	Alexa Fluor 647	BD	Mouse IgG ₁ k
IgG (H+L) F(ab') ₂ Fragment		Alexa Fluor 647	Cell Signaling	Rabbit IgG
CD45	2D1	PerCP	BD	Mouse IgG ₁ k
CD7	8H8	ECD (Phycoerythrin-Texas Red)	Beckman Coulter	Mouse IgG _{2a}
CD127	A019D5	PE-Cy7	BioLegend	Mouse IgG ₁ k
CD132	TUGh4	PE	eBioscience	Rat IgG _{2b} λ
anti p-4E-BP1 (Thr37/46)	236B4	Alexa Fluor 488	Cell Signaling	Rabbit IgG
anti p-AKT (T308)	D25E6		Cell Signaling	Rabbit IgG
anti PTEN	A2B1	PE (Phycoerythrin)	BD	Mouse IgG ₁ k
anti p-AKT (S473)	D9E	Alexa Fluor 647	Cell Signaling	Rabbit IgG
anti p-S6 (pS235/pS236)	D57.2.2E	Alexa Fluor 647	Cell Signaling	Rabbit IgG
anti p-STAT3 (pY705)	4/P-STAT3	Alexa Fluor 488	BD	Mouse IgG _{2a} k
anti p-STAT5 (pY694)	47/Stat5	Alexa Fluor 647	BD	Mouse IgG ₁ k

Cells were acquired on a FACSaria™ flow cytometer (BD) equipped with 488-nm, 633-nm and 405-nm lasers. Data (at least 100,000 events per tube) were collected and analyzed as previously described (33) using the DIVA™ software (BD). Primary T-ALL samples that did not reach at least 25% of IL7-inducible pSTAT5 response in residual T cell were excluded from subsequent analyses. Histograms overlays was carried out by FlowJo® Software. Leukemic cells and normal residual T-cells were identified by using CD7-ECD and CD45-PerCP antibodies as shown in **Supplementary Figure 2 panel A and B**.

Positivity threshold for phosphoprotein expression was established by the comparative use of isotype IgG instead of the phosphoprotein specific antibody (**Supplementary Figure 2, panel C**). Basal level of each phosphoprotein was then calculated as percentage (%) of phosphoprotein positive (p-positive) cells in unstimulated conditions. Response to each cytokine was calculated as percentage of p-positive cells after exposure to cytokine minus the percentage of p-positive cells in the basal state. IL7 inducible pSTAT5 signaling in residual normal T cells contained within the primary leukemia samples was considered as positive control of functional signaling.

Supplementary Figure 2



Western Blotting

Cells were thawed and collected by centrifugation, washed twice in ice-cold phosphate buffered saline (PBS), and pellets were lysed for 30 minutes at 4°C in RIPA-buffer (Tris-HCl pH 7.4 20mM, NaCl 20mM, EDTA pH8 2mM, Na₃VO₄ 0.2mM, Triton 1%, NaF 25mM, β-glycerolphosphate 25mM), with protease inhibitor cocktail supplemented with 1 mM phenylmethylsulphonyl fluoride (PMSF) to inhibit phosphoproteins. Homogenates were centrifuged 14,000 x g for 10 minutes 4°C and supernatants were stored at -80°C. Protein concentration was determined with Bradford protein Assay (Sigma-Aldrich, St. Louis, MO, USA). Twenty micrograms of proteins were resolved on an Any kD precast polyacrylamide gel and transferred onto polyvinylidene difluoride (PVDF) membranes. Nonspecific binding sites were blocked by incubation in blocking buffer, 1X tris buffered saline (TBS) containing 0.1% tween-20 (TBS/T) and supplemented with 10% bovine serum albumin (BSA) for 2 hours at room temperature. After three TBS/T washes, membranes were incubated with primary antibodies overnight at 4°C in TBS/T with 5% BSA. Then, membranes were washed and incubated with peroxidase conjugate secondary antibodies diluted in TBS/T for 1 hour at room temperature. A StripAblot Stripping Buffer (Euroclone S.p.A., Pero, Italy) was used to recover membranes. Antigens were revealed using Clarity Western Luminol/Enhancer solution and peroxide solution (Clarity Western ECL Substrate BIO-RAD) by Alliance Instrument (Uvitec Software). Densitometry analyses were performed using Uviband Software (Uvitec, Cambridge, UK). The following antibodies were used: rabbit anti-PTEN antibody used at working dilution 1:1000 (Cell Signaling Technology) and rabbit anti-beta Actin (D6A8) antibody at 1:1000 (Cell Signaling Technology) to evaluate the quality of protein extracts and goat anti-Rabbit IgG (H+L) (human IgG absorbed); horseradish peroxidase conjugate (BIO-RAD) used at 1:3000. Positivity or negativity was established by assessing the presence or absence of protein bands.

Patients' DNA samples for PTEN Exon7 mutation

Genomic DNA samples were collected from primary T-ALLs samples. Sequencing of PTEN exon 7 was performed by PCR amplification, and PCR products were directly sequenced in both directions using Applied Biosystems ABI PRISM-3130 Genetic Analyzer instrument (Life Technologies). Alignment was carried out using the Basic Local Alignment Search Tool database (BLAST, www.blast.ncbi.nlm.nih.gov). Genomic DNA samples were screened for the type 1 and type 2 TAL1 deletions by PCR amplification using BIOMED-1 primer sets and PCR conditions [42].

Statistical analysis

Statistical analyses, as defined in each figure legend, were performed using Prism V6.0 (GraphPad, La Jolla, CA, USA). The *t*-test was used to compare the continuous variables relative to proteins and phosphoproteins expression levels as assessed by FC and by phosphoflow. A *p*-value of 0.05 was used as the cut-off below which results were considered statistically significant.

RESULTS

Expression of CK2, MYC and ERG in T-ALL cases

We preliminarily screened 26 patients with T-ALL for diagnostic molecular characterization and we found five cases with *PTEN-Exon7* mutation (19%), three with *PICALM/MLLT10* rearrangement (11.5%), seven with *TLX3 (HOX11L2)* alteration (27%), one *TP53* mutated (4%), sixteen with *CDKN2A* deletion (61.5%), six *CRLF2* overexpressed (23%) and three out of 20 patients with *IKZF1* deletion (15%) respectively (**Table Results 1**).

Table Results 1. Genetic alterations according to Final risk group in 26 childhood T-ALL patients

	Non-HR n=15 n(%)	HR* n=11 n(%)	Total n=26 n(%)
<i>PTEN Exon7 deletion or inactivating mutations</i>			
Negative	13 (86.7)	8(72.7)	21 (80.8)
Positive	2 (13.3)	3 (27.3)	5 (19.2)
<i>PICALM/MLLT10</i>			
Negative	14 (93.3)	9 (81.8)	23 (88.5)
Positive	1 (6.7)	2 (18.2)	3 (11.5)
<i>TLX3/HOX11L2</i>			
Negative	8 (53.3)	11 (100)	19 (73.1)
Positive	7 (46.7)	-	7 (26.9)
<i>CDKN2A Δ</i>			
Negative	4 (26.7)	3 (27.3)	7 (26.9)
Positive	10 (66.7)	6 (54.5)	16 (61.5)
Not performed ^o	1 (6.6)	2 (18.2)	3 (11.6)
<i>IKZF1 Δ</i>			
Negative	10 (66.7)	7 (63.6)	17 (65.4)
Δ1-3	-	2 (18.2)	2 (7.7)
Δ1-8	1 (6.6)	-	1 (3.8)
Not performed ^o	4 (26.7)	2 (18.2)	6 (23.1)
<i>hi-CRLF2</i>			
Negative	9 (60)	10 (90.9)	19 (73.1)
Positive	5 (33.3)	1 (9.1)	6 (23.1)
Not performed ^o	1 (6.7)	-	1 (3.8)

Table Legend: *according to Final risk group; ^oNot performed: not enough samples availability.

Firstly, we compared *CK2* expression in T-ALL cases to HDs and CEM cell line, showing a similar finding between T-ALL and CEM (**Figure Results 1A**). Then we observed a statistically significant difference of *CK2* expression in T-ALL patients vs HDs (**Figure Results 1B**). We point out that 10 out of 11 HR-T-ALL patients (90%) presented *CK2* mRNA expression up to 5 times higher than HDs and 2 times higher than other T-ALL. Moreover, 4 out of five *PTEN Exon7* mutated cases showed a high *CK2* mRNA level (**Figure Results 2**). Furthermore, we correlated *CK2* expression among cases with *CDKN2A*, *IKZF1* deletions and *CRLF2* overexpression, respectively. We found out that children with *IKZF1* and *CDKN2A* deletions showed high *CK2* mRNA levels, although it was not statistically significant (**Figure Results 3A and 3B**). We did not find any difference in *CK2* expression among cases with *CRLF2* overexpression compared with normal *CRLF2* expression (**Figure Results 3C**).

Figure Results 1A. *CK2* mRNA expression in CEM-cell line was comparable with T-ALLs (mean fold change 5.040 Vs 4.129, respectively) Vs HDs (mean fold change 1.244)

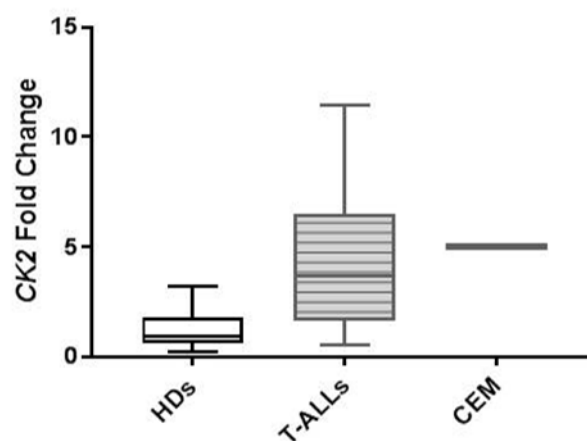


Figure Results 1B. Statistically significant difference of Ck2 expression in T-ALL (range fold change: 0.546-11.471) Vs HDs (range fold change: 0.350-2.180) (p=0.0031)

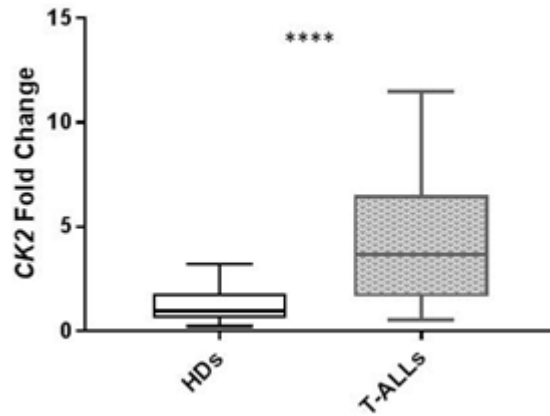


Figure Results 2 Four out of 5 PTEN *Exon7* mutated T-ALL patients showed high CK2 mRNA level (mean=5.621) though it was not significantly different between PTEN-wt and mutated samples. CK2 expression was statistically different comparing both PTEN *Exon7* wild type and mutated patients to healthy donors

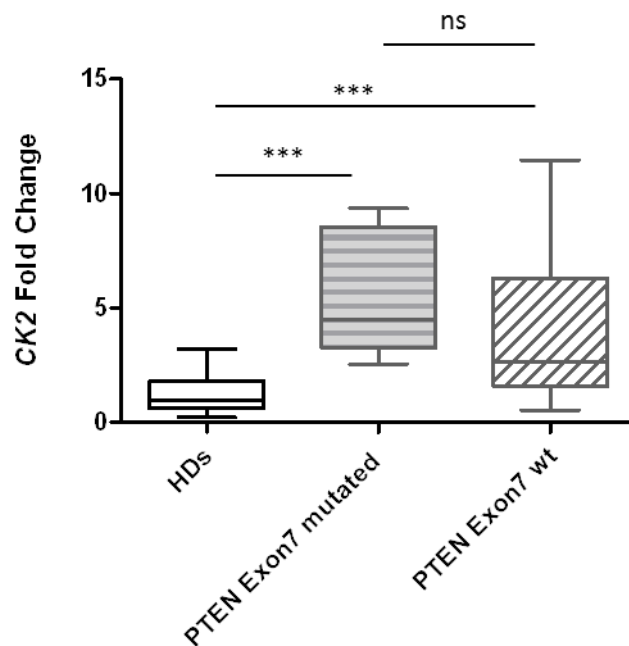
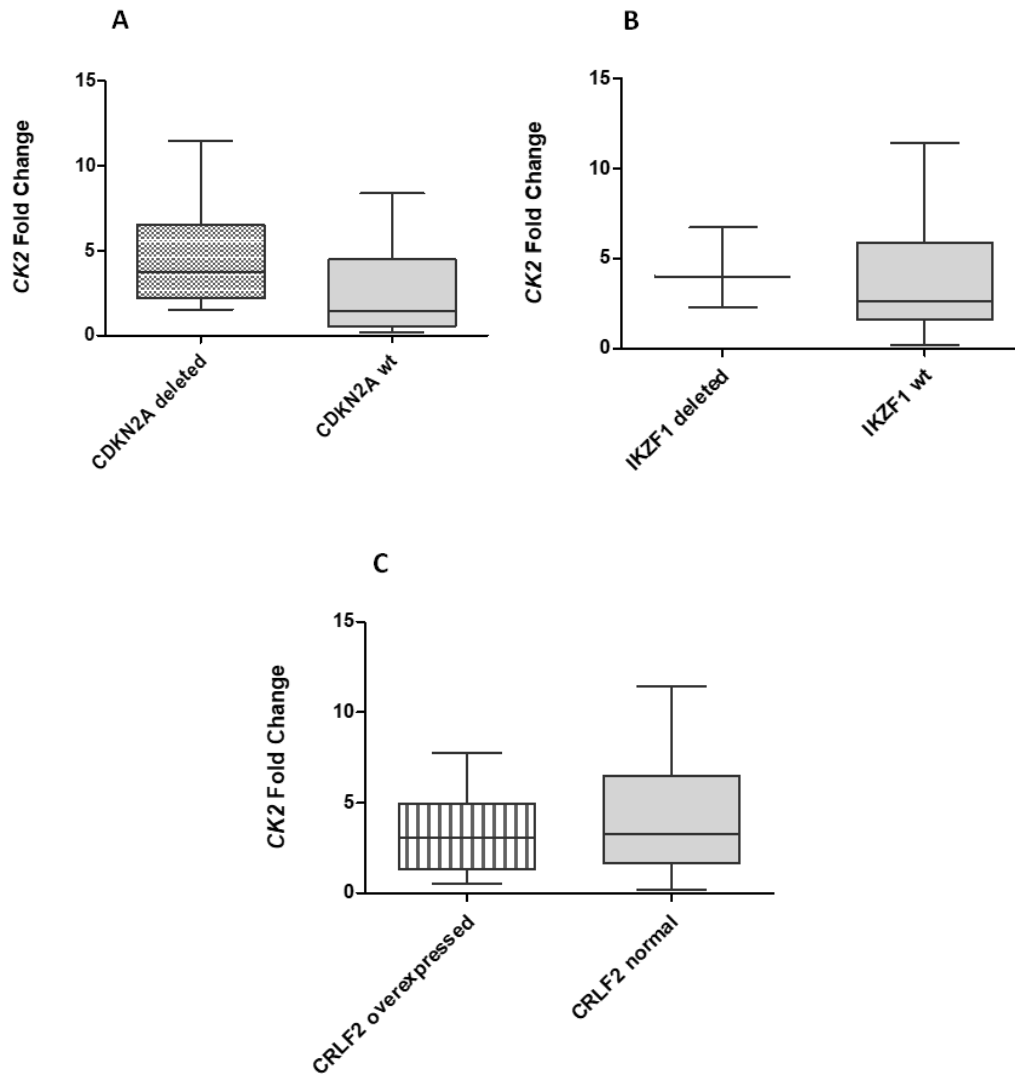


Figure Results 3 The sixteen *CDKN2A* deleted patients (A) and the three *IKZF1* deleted patients (B) showed high *CK2* mRNA levels, although data is not statistically significant (Median *CK2* *CDKN2A* deleted 3.737 Vs Median *CK2* *CDKN2A* wild type 1.418; Median *CK2* *IKZF1* deleted 4.000 Vs Median *CK2* *IKZF1* wild type 2.626). We did not find any difference about *CK2* expression among *CRLF2* overexpressed and normal expressed (Median 3.061 Vs 3.279) (C).

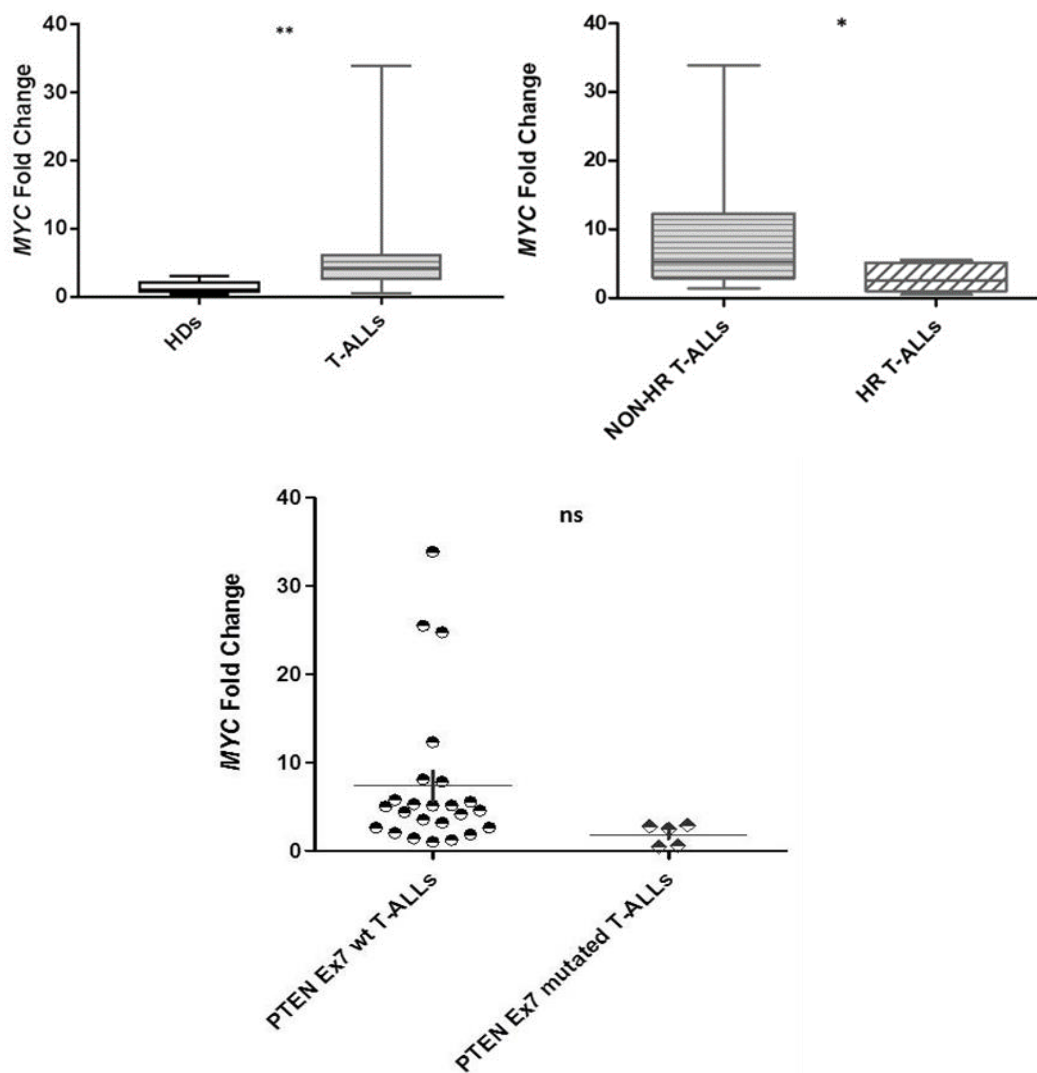


MYC expression in the CEM-cell line was exactly comparable with T-ALLs. We observed a statistically significant difference of *MYC* expression in children with T-ALL than HDs (**Figure Results 4A**). Comparing T-ALL with HDs *MYC* expression, we identified thirteen out of 26 T-ALL

patients as *MYC-high* (50%): five HR and eight non-HR, respectively. Seven out of 8 *MYC-high* non-HR patients showed a *TLX3 (HOX11L2)* rearrangement. Overall, we observed a statistically significant difference of *MYC* expression between HR and non-HR T-ALLs (**Figure Results 4B**).

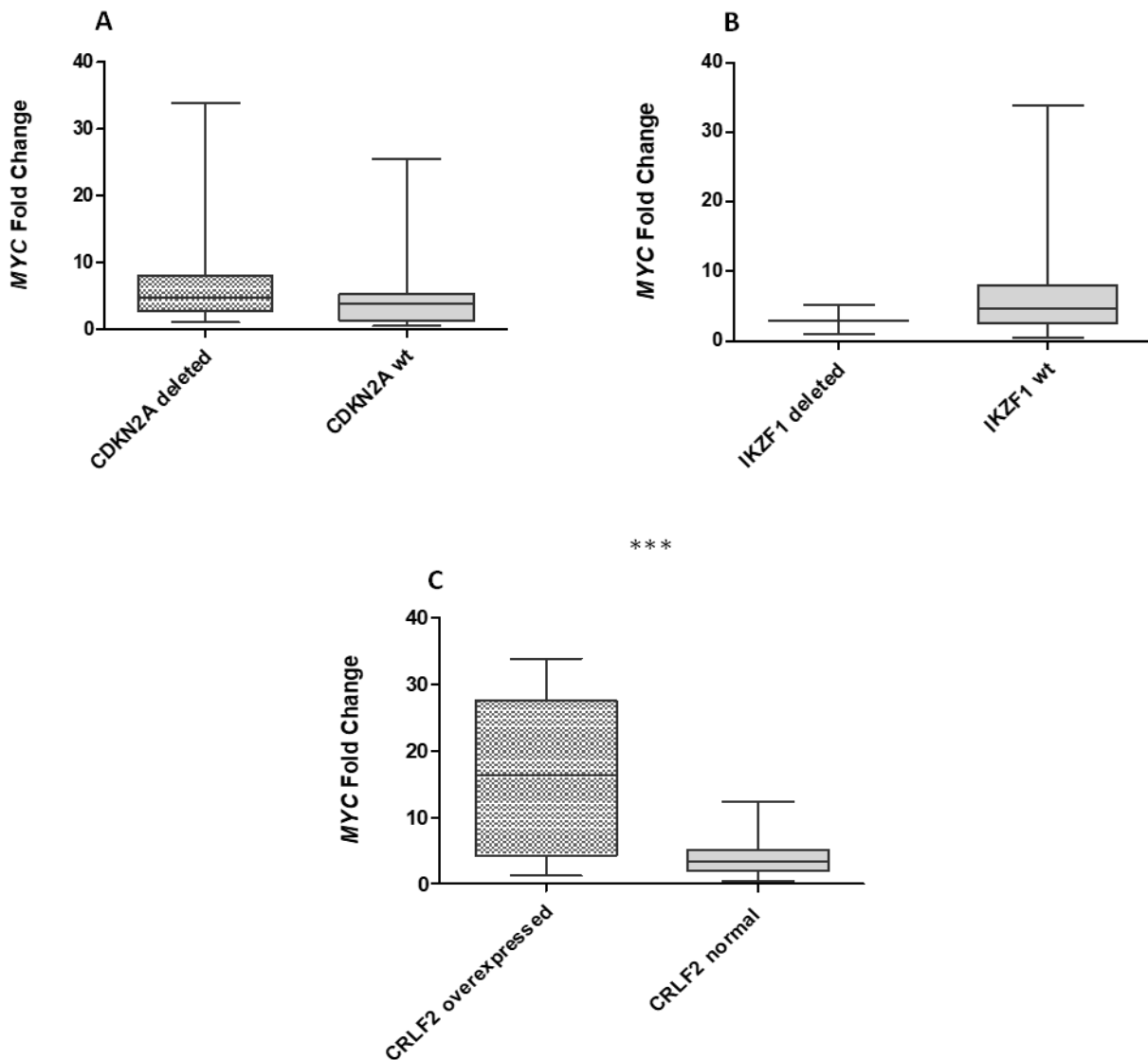
In *PTEN-Exon7* mutated patients, we observed a low expression of *MYC* (**Figure Results 4C**).

Figure Results 4: We observed a statistically significant difference of *MYC* expression in children with T-ALL than HDs ($p=0.019$) *MYC* expression in 26 children with T-ALL resulted higher than in HDs: Mean Fold Change (MFC) 6.802 (range 0.475-33.855) vs 1.280 (range 0.298-2.966) respectively (**A**); *MYC* MFC expression was statistically different between non-HR and HR T-ALL patients (9.596 Vs 2.992 respectively) (**B**). Moreover *PTEN Exon7* mutated patients showed a low expression of *MYC* compared to *PTEN* wild-type: MFC 1.838 (range 0.475-2.871) vs 7.984 (**C**)



Moreover, we compared *MYC* expression with *CDKN2A* e *IKZF1* status and we did not observe any statistically significant difference of *MYC* expression (**Figures Results 5A and 5B**). By contrast, in T-ALL cases with a high *CRLF2* expression we detected a very high *MYC* expression compared to cases with normal *CRLF2* expression (**Figure Results 5C**). Five out of the 6 *CRLF2* overexpressed cases had a *TLX3* rearrangement.

Figure Results 5: We did not observe any statistically significant *MYC* expression difference between both *CDKN2A* and *IKZF1* deleted and wild type patients (**A** and **B**). By contrast, comparing *CRLF2* expression to *MYC* expression, we interestingly saw that *CRLF2* overexpressed patients shown higher *MYC* expression than *CRLF2* normal expressed (mean FC *MYC* expression 16.404 Vs 3.921, respectively) (**C**)



ERG expression in CEM-cell line was very low, compared to HDs and T-ALL cases, respectively (data not shown). We then analyzed *ERG* mRNA level in children with T-ALL vs HDs showing a statistically significant different expression (**Figure Results 6A**). Ten out of 26 T-ALLs (38.5%) were *ERG-high* with *ERG* MFC expression of 67.060 [8 HR cases and 2 non-HR]. The difference of *ERG* expression between the two T-ALL subgroups was not statistically significant (**Figure Results 6B**). When we analyzed the five T-ALLs with *PTEN Exon7* mutation, they showed slightly higher levels of *ERG* mRNA than *PTEN Exon7* wild type patients (**Figure Results 6C**). Moreover, we analyzed thymocytes as normal internal control about *CK2*, *MYC* and *ERG* expression comparing with HDs. *CK2* expression was absolutely comparable between thymocytes and HDs. Instead, MFC *MYC* expression in thymocytes was comparable to T-ALL samples. This is due to an overlapping metabolic rewiring in activated T-cells and *MYC*-transformed lymphocytes similar to what happens in tumor cells (with the activation of proto-oncogenes such as c-Myc) [43]. *Erg* expression was comparable in thymocytes and HDs too (**Table Results 2**).

Figure Results 6: *ERG* mRNA level in pediatric T-ALL was really higher than HDs *ERG* levels (mean T-ALL 38.497 Vs mean HDs 2.605) (A); The difference of *ERG* expression between the two T-ALL subgroups (HR mean 45.838 Vs NON-HR mean 33.114) was not statistically significant (B)

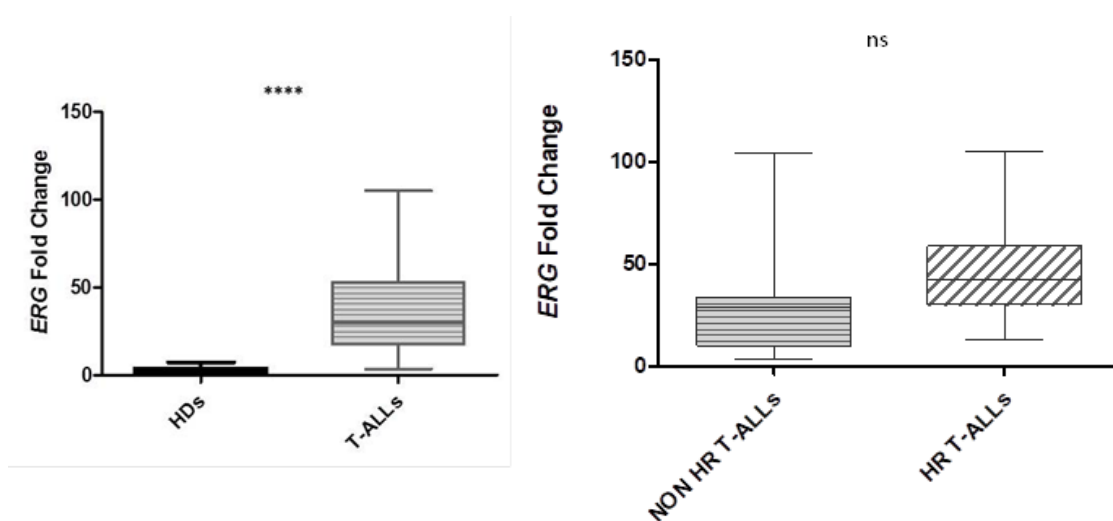


Figure Results 6C: The five T-ALLs PTEN Exon7 mutated showed slightly higher levels of ERG mRNA (mean 41.973 Vs 38.052)

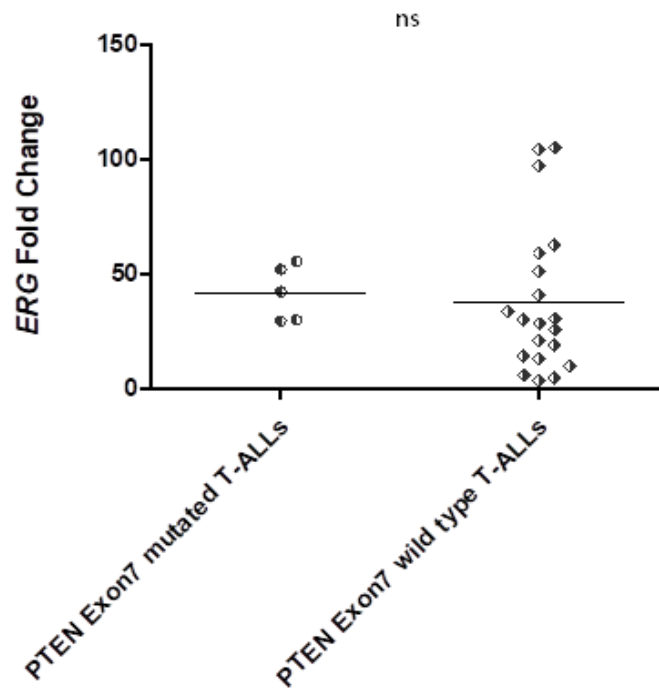


Table Results 2

	CK2 expression		MYC expression		ERG expression	
	<i>Range</i>	<i>Mean/Median</i>	<i>Range</i>	<i>Mean/Median</i>	<i>Range</i>	<i>Mean/Median</i>
Thymocytes	-	1.100 / 1.100	-	5.800 / 5.800	-	5.670 / 5.670
Healthy Donors	0.220-3.180	1.237 / 0.955	0.298-2.966	1.280 / 0.970	0.222-7.438	2.605 / 2.124
T-ALL	0.546-11.471	4.286 / 3.911	0.475-33.855	6.802 / 4.263	3.372-105.164	38.947 / 30.077
B-ALL	0.499-5.489	3.011 / 2.777	0.326-15.807	2.881 / 1.925	2.981-477.713	191.977 / 180.995

Expression of CK2, MYC and ERG in B-ALL cases

We screened 35 B-ALL patients, stratified in four biological subgroups according to the most common molecular alterations detected at diagnosis of pediatric B-ALL (**Table Results 3**).

In this subgroup we performed *CK2* expression analysis, observing a statistically significant difference of *CK2* expression in B-ALL patients respect to HDs (**Figure Results 7A**). *CK2* expression resulted homogenous among the four selected biological ALL subgroups, as shown in **Figure Results 7B**. In the entire cohort of B-ALL cases, we found a statistically significant difference of *MYC* expression respect to HDs (**Figure Results 8A**). Interestingly, we observed a correlation between *MYC* expression with a prognostic genetic subgroup: in the Ph+ cases, *MYC* expression was high whereas in t(12;21) pos B-ALL was low. In the latter subgroup, two cases, who subsequently presented a late relapse, showed a higher value of *MYC* expression. Moreover, in 7 out of 7 HR in the “B-others” subgroup we detected high *MYC* expression as well as we observed in four cases included in the *MLL*-R B-ALL subgroup (**Figure Results 8B**). In cases with B-ALL, we also observed a high level of *ERG* expression compared with HDs (**Figure Results 9A**). These values were higher than *ERG* expression findings in T-ALLs. Among different biological subgroups, *ERG* expression was higher in t (12;21) pos ALL than Ph+, B-others and particularly *MLL*-R B-ALL (**Figure 9B**). This inverse correlation with clinical risk was confirmed by the fact that 84% of HR B-ALL cases showed a low expression of *ERG*.

Summary of *CK2*, *MYC* and *ERG* expression according to genetic alterations in children with T- and B-ALL is featured in **Table Results 4** while their expression according Final Risk are shown in **Table Results 5**.

Table Results 3: Genetic alterations according to *Final risk group* in 35 childhood B-ALL patients

	Non-HR n=16 n(%)	HR* n=19 n(%)	Total n=35 n(%)
<i>BCR/ABL1</i>			
Negative	16 (100)	11 (58)	27 (77)
Positive	-	8 (42)	8 (23)
<i>ETV6/RUNX1</i>			
Negative	-	19 (100)	19 (100)
Positive	16 (100)	-	16 (100)
<i>MLL rearranged</i>			
Negative	16 (100)	15 (79)	31 (89)
Positive	-	4 (21)	4 (11)
<i>“Others” (without known translocations)</i>			
		7 (36.8)	7 (20)
<i>CDKN2A-Δ</i>			
Negative		5 (71)	5 (71)
Positive		2 (29)	2 (29)
<i>IKZF1-Δ</i>			
Negative		5 (71)	5 (71)
Positive		2 (29)	2 (29)
<i>hi-CRLF2</i>			
Negative		5 (71)	5 (71)
Positive		2 (29)	2 (29)

Figure 7: Ck2 mRNA level higher in B-ALL than HDs (mean CK2 fold change 3.076 Vs 1.236 respectively) (p=0.0003) (A); Ck2 overexpression does not seem to be correlated with the final risk (NON-HR and HR B-ALLs). The expression was homogeneous among the four subgroups (B)

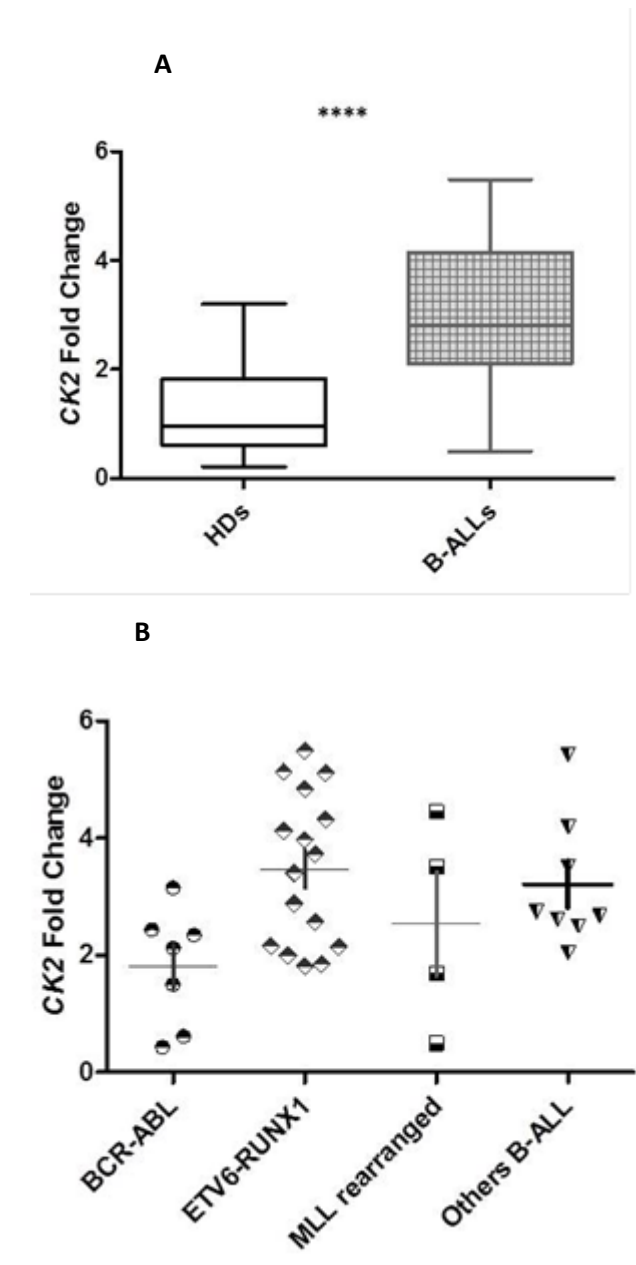


Figure 8: Statistically significant difference of *c-Myc* expression in B-ALL patients than HDs (mean fold change 2.887 Vs 1.284, $p= 0.005$) (A); Significant difference of MYC expression correlated with final risk in B-ALLs (lower levels in 12;21 B-ALLs and very higher levels in q23 rearranged B-ALLs): all *c-MYC-high* B-ALL patients were HR as final risk or had any event (B)

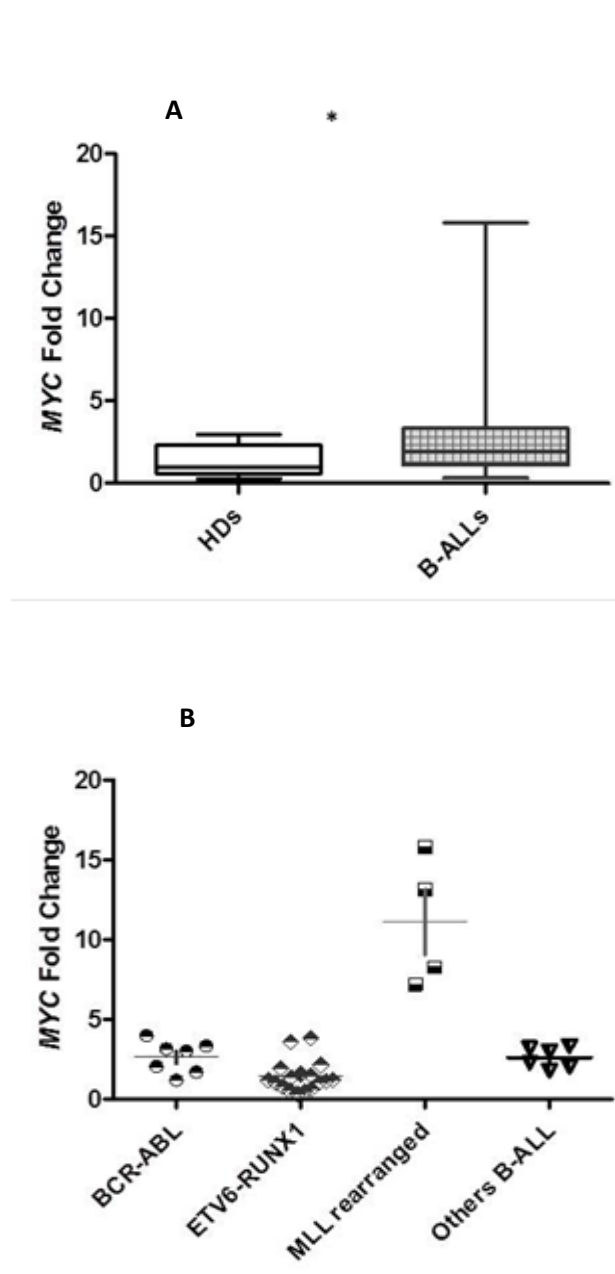


Figure 9: *ERG* mRNA expression in B-ALLs was very higher compared to HDs expression value (mean 191.770 Vs mean HDs 2.605) (A); *ERG* overexpression could be not correlated with poor prognosis: data show high *ERG* levels in t (12;21) B-ALLs than *ERG* expression level of the other subgroups (B)

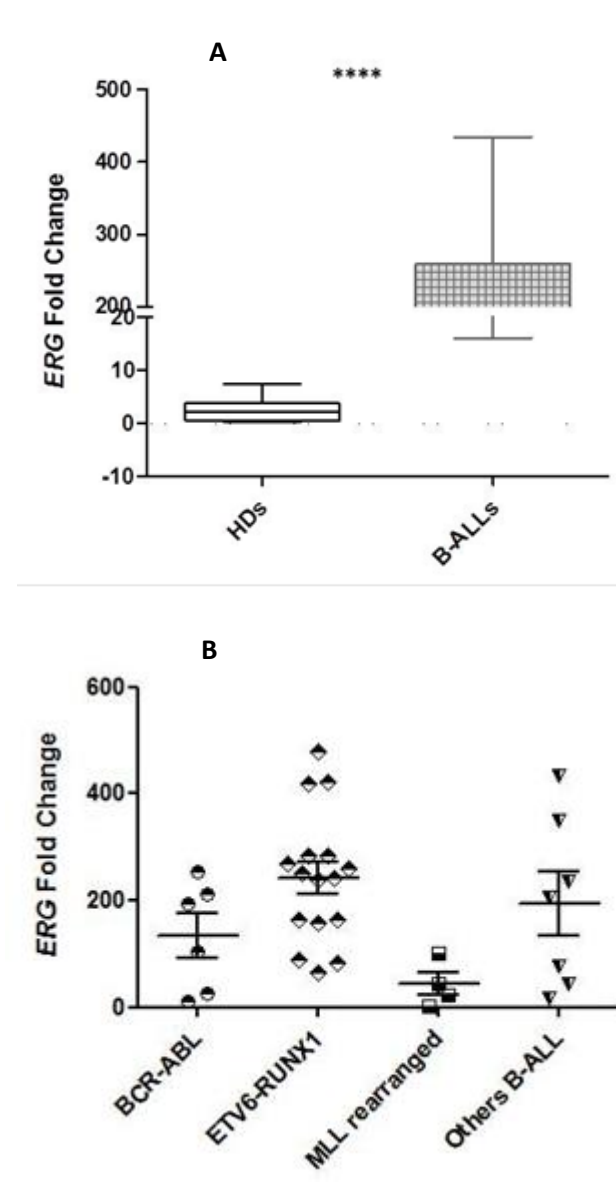


Table Results 4: *CK2*, *MYC* and *ERG* expression according to genetic alteration in T-ALL and B-ALL patients

Genetic Alteration	Analyzed patients	<i>CK2</i> expression		<i>MYC</i> expression		<i>ERG</i> expression		
		Low n(%)	High n(%)	Low n(%)	High n(%)	Low n(%)	High n(%)	
<i>BCR/ABL1</i>	B-ALL (n= 8/35)	3 (37.5)	5 (62.5)	1 (12.5)	7 (87.5)	6 (75)	2 (25)	
<i>ETV6/RUNX1</i>	B-ALL (n= 16/35)	8 (50)	8 (50)	14 (87.5)	2 (12.5)	6(37.5)	10 (62.5)	
<i>MLL rearranged</i>	B-ALL (n= 4/35)	2 (50)	2 (50)	-	4 (100) ^o	4 (100) ^a	-	
<i>PTEN Exon7 Δ or inactivating mutations</i>	T-ALL (n= 5/26)	2 (40)	3 (60)	5 (100)	-	1 (20)	4 (80)	
<i>PICALM/MLLT10</i>	T-ALL (n= 3/26)	2 (67)	1(33)	1 (33)	2(67)	1 (33)	2(67)	
<i>TLX3/HOX11L2</i>	T-ALL (n= 7/26)	3(43)	4(57)	-	7(100) ^o	5(71.5)	2(28.5)	
O T H E R S	<i>CDKN2A Δ</i>	B-ALL (n= 2/7)	2 (100)	-	-	2 (100)	2 (100)	-
		T-ALL (n= 16/23)	8(50)	8(50)	7(44)	9(56)	8(50)	8(50)
	<i>IKZF1 Δ</i>	B-ALL (n= 2/7)	2 (100)	-	-	2 (100)	2 (100)	-
		T-ALL (n= 3/20)	-	3(100)	2(67)	1(33)	-	3(100)
	<i>hi-CRLF2</i>	B-ALL (n= 2/7)	1 (50)	1 (50)	-	2 (100)	1 (50)	1 (50)
		T-ALL (n= 6/25)	3(50)	3(50)	1(47)	5(83)	4(67)	2(33)

^a very LOW *ERG* expression ; ^o very HIGH *MYC* expression

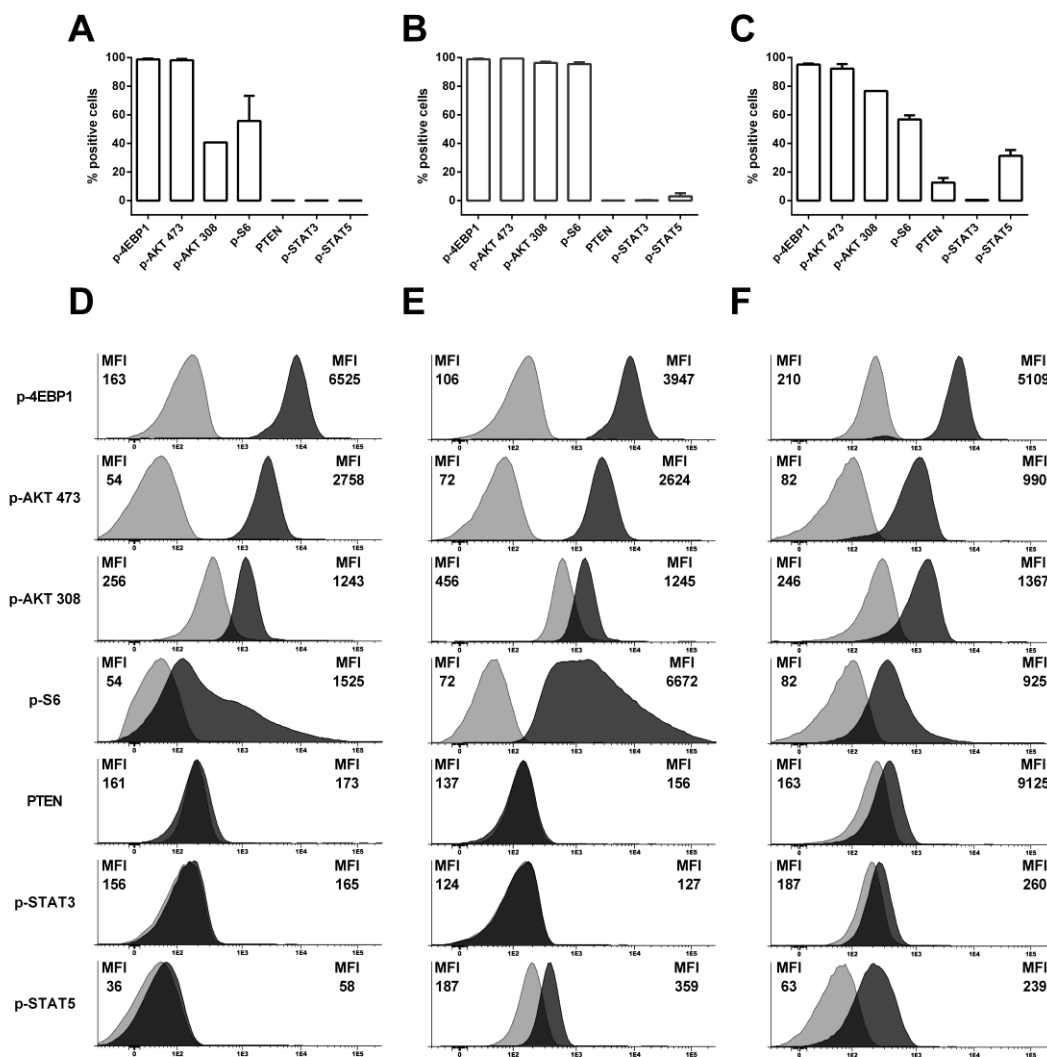
Table Results 5: *CK2*, *MYC* and *ERG* expression according to *Final risk group* in T-ALL and B-ALL patients

		<i>CK2</i> expression		<i>MYC</i> expression		<i>ERG</i> expression	
		<i>Low</i> n(%)	<i>High</i> n(%)	<i>Low</i> n(%)	<i>High</i> n(%)	<i>Low</i> n(%)	<i>High</i> n(%)
T-ALL	NON-HR (n= 15)	9 (60)	6 (40)	7 (47)	8 (53)	11 (73)	3 (27)
	HR (n= 11)	2 (18)	9 (82)	6 (54.5)	5 (45.5)	2 (19)	9 (81)
B-ALL	NON-HR (n= 16)	8 (50)	8 (50)	14 (87.5)	2(12.5)	6 (37.5)	10 (62.5)
	HR (n= 19)	8 (42)	12 (58)	2 (10.5)	17 (89.5)	15 (79)	4 (21)

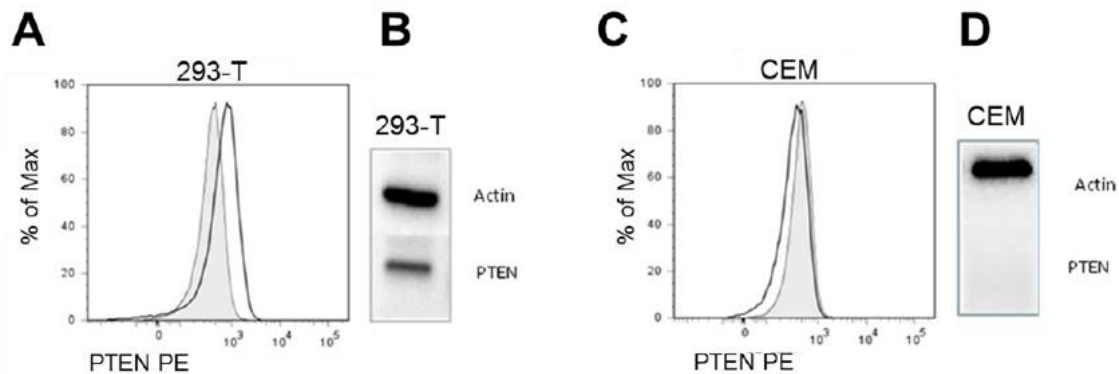
PI3K and JAK/STAT basal signaling in T-ALL cell lines

We first performed a basal level phosphoflow assay in CEM, Jurkat and HPB-ALL cell lines carrying different *PTEN* status. After starvation in X vivo the mean cell viability observed for all experiments was >90%. We observed a constitutive hyperactivation of the PI3K pathway in all the analyzed cell lines. Moreover, we assessed the basal level of phosphorylated JAK/STAT downstream targets and found elevated levels of pSTAT5 only in HPB-ALL cell line ($31.3\pm 4.1\%$), whereas pSTAT3 was inactive in all tested cell lines. PTEN protein expression was detected in HPB-ALL *PTEN* wild-type (*wt*) cell line ($56.8\pm 3.0\%$), whereas it was not expressed neither in CEM nor in Jurkat cells due to their *PTEN* genetic mutation (**Figures Results 10, panels A, B, C**). Mean Fluorescence Intensity (MFI) was also evaluated as shown in panels **D, E** and **F** of Figure 10. To determine PTEN expression levels, we carried out phosphoflow and WB analyses in parallel experiments using CEM and 293T cells as negative and positive control respectively. As shown in **Supplementary Figure 3**, regardless of the method employed, 293T cells tested positive for PTEN expression, whereas CEM cells were PTEN negative.

Figure Results 10: Constitutive PI3K and JAK/STAT signaling in T-ALL cell lines with different status of PTEN. Basal expression measured by phosphoflow. in three T-ALL cell lines representative of different status of PTEN gene, percentages are indicated in boxplots and MFI in histograms respectively: CEM (panel A and D) JURKAT (panel B and E), and HPB-ALL (panel C and F). PTEN protein was not expressed neither in CEM nor in JURKAT cells due to their PTEN exon 7 mutation, whereas it is expressed in PTEN wt HPB-ALL cells. A constitutive hyperactivation of p4EBP1, pAkt473, pAkt308, and pS6 phosphoproteins is observed in all cell lines. JAK/ STAT basal pathway is generally not activated with the exception of HPB-ALL cell line with partial pSTAT5 expression.



Supplementary Figure 3: Comparison between phosphoflow and Western Blotting methods in T-ALL cell lines. PTEN expression as assessed by phosphoflow and WB analyses in parallel experiments using 293T and CEM cells as positive and negative control respectively; Gray histograms represent the fluorescence of cells stained with isotype IgG (negative control), open histograms represent the fluorescence of cells stained with the specific anti-PTEN antibody. Phosphoflow (panels A and C) and WB (panels B and D) provided comparable results in the measurement of PTEN expression using the two methods.



PI3K basal signaling in primary T-ALL samples according to PTEN mutation

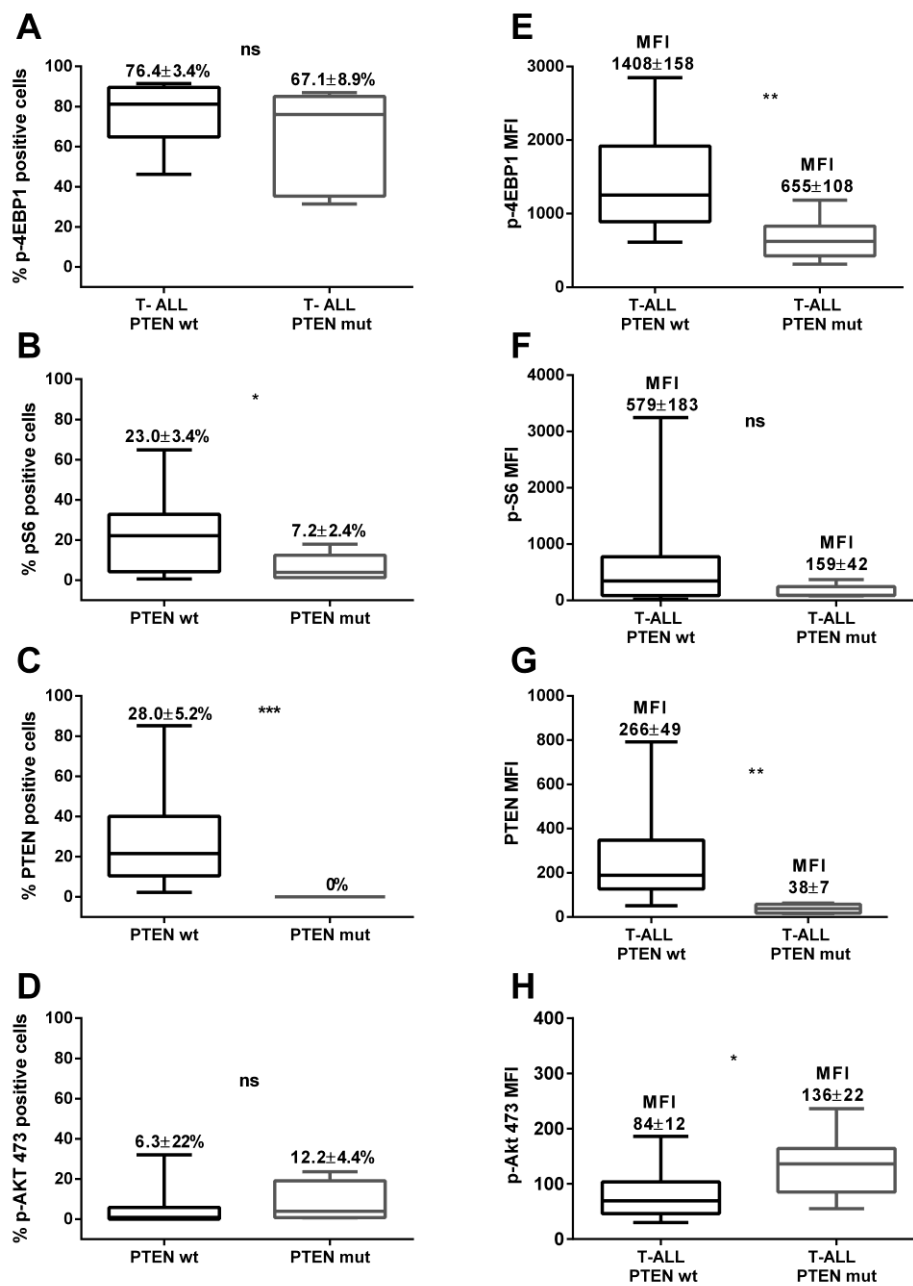
We next sought to determine basal expression level of the PI3K signaling in blasts from 25 primary T-ALL samples and in T cells from 11 normal BM samples. Cell viability of thawed primary cells after X-vivo starvation was 85.2% SD=8.0%, range 70%-95%. Two samples were excluded from the phospho-signaling analyses because they did not meet the predetermined criterion of either $\geq 70\%$ of viable cells or at least 25% of IL7-inducible pSTAT5 response in residual T cell within the T-ALL samples. In this regard samples included in the final analyses showed a mean pSTAT5 response of 48.9% (SD=10.5, range 26.4%- 64.3%). Similarly to cell lines, we found constitutive hyperactivation of the PI3K downstream targets in most of samples (Figure 2). Specifically, we observed that p4EBP1, pS6, pAkt473, and PTEN were all significantly activated as compared to normal BM samples: ($77.8 \pm 3.5\%$ vs $22.0 \pm 3.0\%$, $p < 0.0001$), ($18.6 \pm 3.7\%$ vs $4.5 \pm 1.3\%$, $p < 0.05$),

($7.7\pm 2.0\%$ vs $0.1\pm 0.04\%$, $p<0.01$), and ($20.1\pm 4.5\%$ vs $2.6\pm 0.9\%$, $p<0.05$) respectively. When we analyzed such molecules according to the *PTEN* status we noticed that p4EBP1 was higher in *PTEN wt* as compared to *PTEN* mutated samples although this was significant only when measured as MFI and not as % of positive cells (**Figure Results 11, panels A and E**), similarly a slightly higher hyperactivation of pS6 was observed in *PTEN wt* as compared to mutated samples (**Figure Results 11, panels B and F**). As expected, *PTEN* mutated T-ALL samples did not express PTEN protein (**Figure Results 11, panels C and G**). pAkt S473 was more hyper activated in *PTEN* mutated samples although this difference was significant only by MFI (**Figure Results 11, panels D and H**). Normal residual T cells were detectable in 19 out of 25 T-ALL samples, and indeed they reproduced the signaling pattern observed in T cells derived from normal BM, confirming their reliable use as internal control for comparative phosphoflow analyses. In this regard measurements as % of positive cells or as MFI provided very similar results (**Supplementary Figure 4**).

Yet, we measured PTEN expression using both WB and phosphoflow in parallel on 9 primary T-ALL samples (6 *PTEN wt* and 3 *PTEN* exon 7 mutated); we obtained concordant results confirming that phosphoflow is a reliable and accurate approach to measure PTEN expression in T-ALL (**Figure Results 12**).

Figures Results 11: PI3K constitutive signaling in primary T-ALL cells according to PTEN status.

Basal expression levels of p4EBP1, pS6, PTEN and pAkt473 proteins was measured in T-ALL patients according to *PTEN status* and are reported as both percentages (graphs **A-D**) and MFI values (graphs **E-H**). pAkt S473 was more hyper activated in PTEN mutated samples although this difference was significant only by MFI. By contrast pS6 and p4EBP1 were under expressed in PTEN mutated samples. As expected, *PTEN* mutated T-ALL samples did not express PTEN protein



Supplementary Figure 4: PI3K constitutive signaling in T-ALL patients with different PTEN status and in normal residual T cells. Constitutive signaling in primary T-ALL cells according to their PTEN status and normal residual T cells from T-ALL patients. As expected primary T-ALL blasts show constitutive hyperactivation of the PI3K pathway as compared to their normal T cell counterparts both as percentages (graphs **A-D**) as MFI fold change (graphs **E-H**).

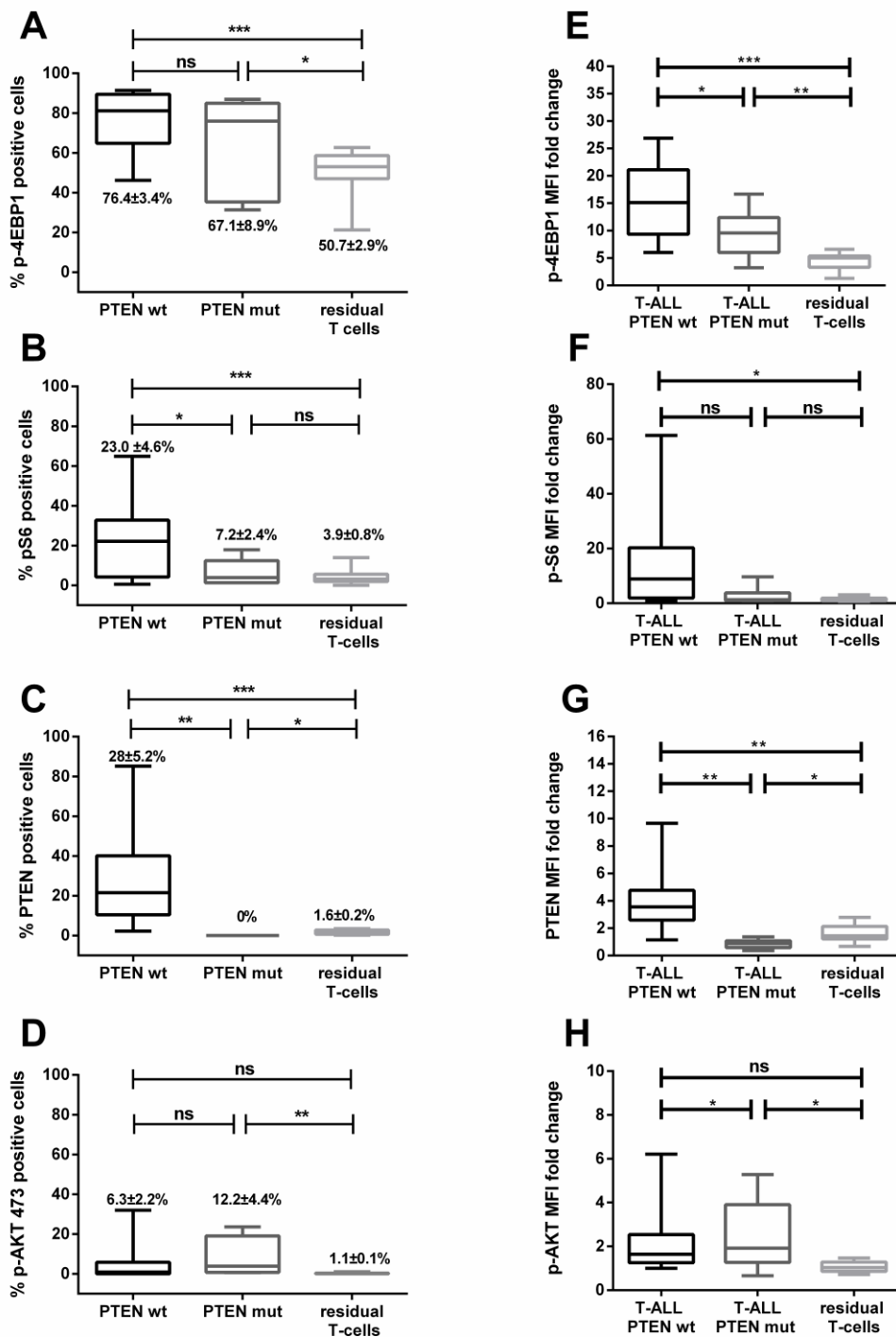
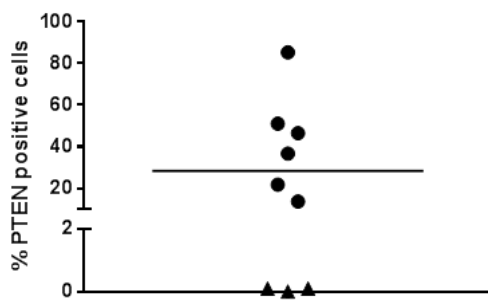
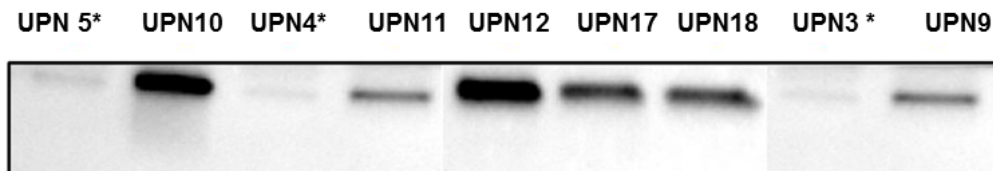


Figure Results 12: Analysis of PTEN expression according to genetic lesion. PTEN protein expression in PTEN exon 7 wt (n 6) and in PTEN exon 7 mutated (n 3) T-ALL patients, as assessed by phosphoflow (panel **A**) and WB (Panel **B**). Panel A shows the % of PTEN-positive cells by phosphoflow. PTEN Exon7 wt and mutated patients are indicated by circles and triangles respectively. Panel B shows the WB analysis: protein bands of each patient are indicated by the individual UPN codes of PTEN wt and mutated (*) patients.

A



B



PI3K signaling inhibition and IL7-induced JAK/STAT pathway activation according to PTEN status.

To measure changes in the basal signaling pathways we used either the dual inhibitor of PI3K pathway NVP-BEZ235 or IL7. As shown in **Figure Results 13**, we observed an inhibition of p4EBP1, pAkt and pS6 phosphorylation in primary T-ALL samples regardless of *PTEN status*. We then assessed the basal phosphorylation levels of STAT5 in 23 T-ALL primary samples (16 *PTEN wt* and 7 *PTEN exon 7 mutated*) as well as in their normal residual T cell compartment. Basal pSTAT5 signal was generally low in both the subgroups ($6.3 \pm 3.5\%$ vs $0.07.x \pm 0.03\%$, $p=ns$ as well as in normal residual T cells ($0.1 \pm 0.09\%$), (**Figure 14, panel A**, dark bars). Exceptions were observed in three patients (all *PTEN wt*): UPN15 carrying NUP214/ABL1 fusion gene (pSTAT5=43.3%), UPN17 carrying ETV6/ABL1 (pSTAT5=33.6%), and UPN24 IL7R mutated (pSTAT5=23.3%). Interestingly, when we assessed IL7-induced pSTAT5 response, all 16 *PTEN wt* T-ALL blasts significantly increased their pSTAT5 expression as compared to basal level (mean= $47.3 \pm 5.3\%$, $p < 0.001$) similarly to the strong response of normal residual T cells (mean= $49.4 \pm 2.4\%$, $p < 0.001$); by contrast, all the *PTEN exon 7 mutated* samples showed a lack or very low pSTAT5 (mean= $6.2 \pm 2.3\%$, p not-significative, **Figure 14 panels A**). This observation was confirmed by measuring MFI of pSTAT5 expressing cells (**Figure 14 panels C**). Regarding the cell lines only *PTEN wt* HPB-ALL cells (mean basal level= $28.3 \pm 6.9\%$,) was able to activate pSTAT5 upon IL7 stimulation (mean= $92.4 \pm 2.8\%$), while *PTEN* deleted or mutated CEM and Jurkat cells were completely non-responsive (mean pSTAT5=0.1% and 3.2% respectively, **Figure 14 panel B**), and assessment by measuring MFI gave similar results (**Figure 14 panel D**).

Figure Results 13: BEZ 235-induced inhibition of PI3K/AKT pathway. BEZ inducible PI3K/Akt signaling was measured in both primary T-ALL PTEN exon 7 mutated and wt cells. Values are expressed as mean values of MFI log₂ ratio (inhibited/basal state) for p4EBP1 (panel A), pAkt473 (panel B) and pS6 (panel C). BEZ abrogates phosphorylation below basal levels regardless of PTEN status.

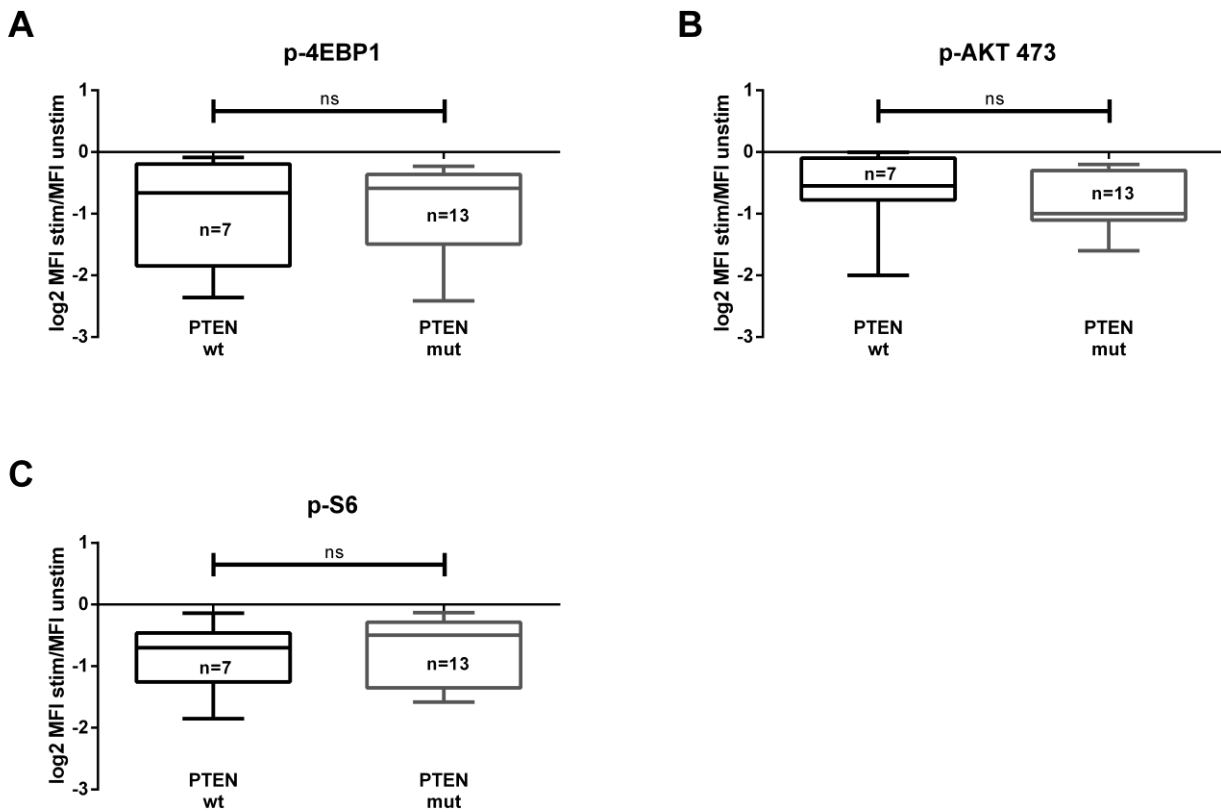
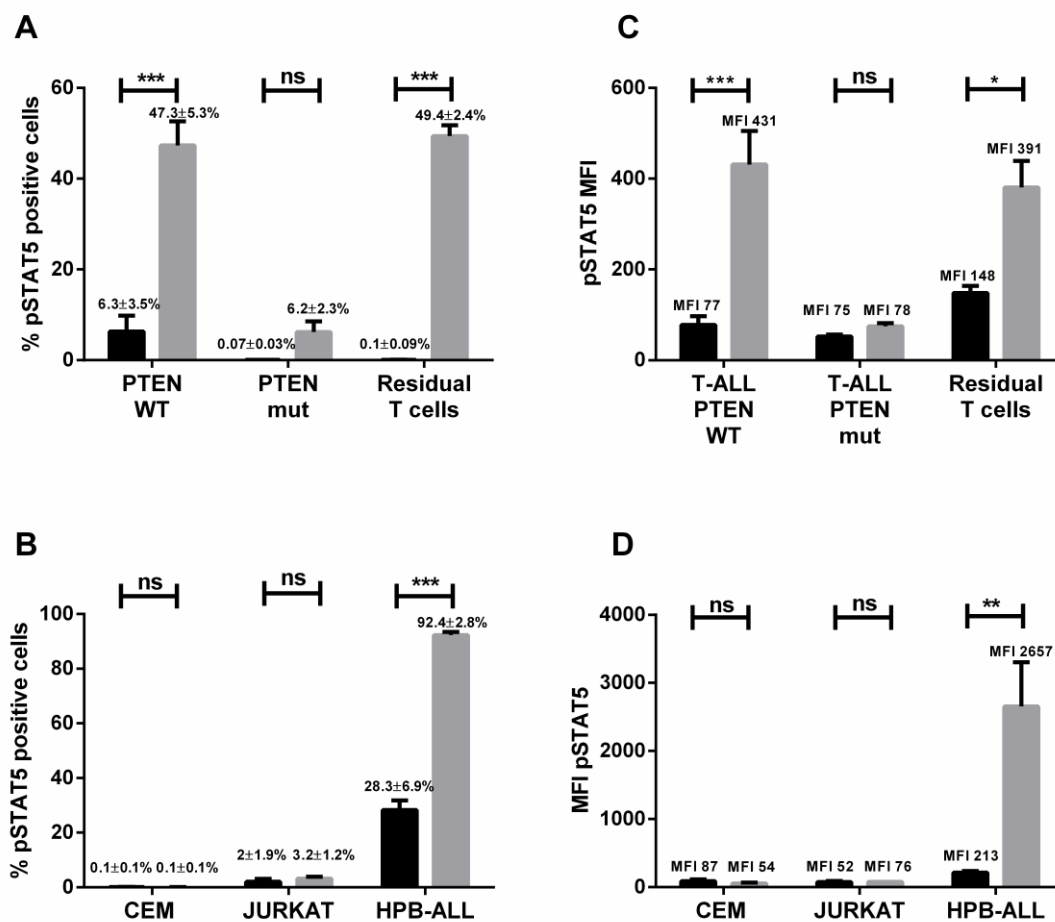


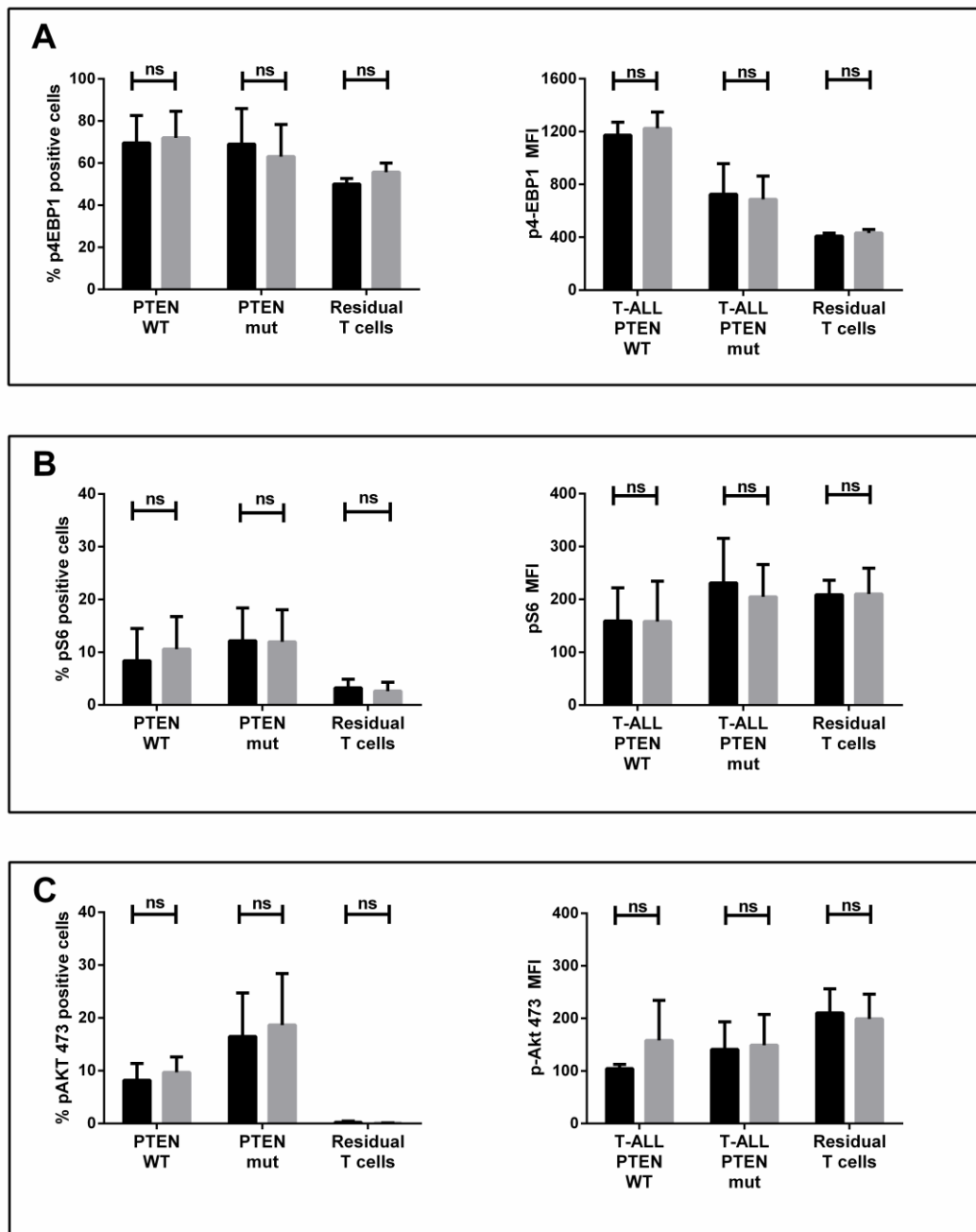
Figure Results 14: Constitutive and IL7 inducible PI3K/Akt and JAK/STAT5 pathways. Panel A and C: At basal state (black bars), STAT5 was not phosphorylated in T-ALL samples regardless of PTEN status with the exception of three PTEN wt patients (UPN 15, UPN 17 and UPN 24) due to their genetic mutation. When IL7 stimulated (grey bars), all of 16 T-ALL PTEN wt samples increased STAT5 phosphorylation significantly. By contrast PTEN mutated patients were low or non-responsive. These trends are consistent as both percentages and as MFI values. IL7 inducible pSTAT5 signaling in residual normal T cells was considered as positive control of functional IL7 driven pSTAT5 signaling. Panel B and D: T-ALL cell lines CEM and Jurkat (both PTEN mutated) and HPB-ALL PTEN wt cell lines provided similar pSTAT5 responses in term of percentages and MFI values as per the primary counterparts.



Regarding IL7-induced PI3K signaling response we studied the p4EBP1, pS6, and pAkt components in 6 T-ALL samples (3 T-ALL *PTEN* wt and 3 *PTEN* mutated samples) including normal residual T cells in the analysis. We did not observe any significant activation neither in T-

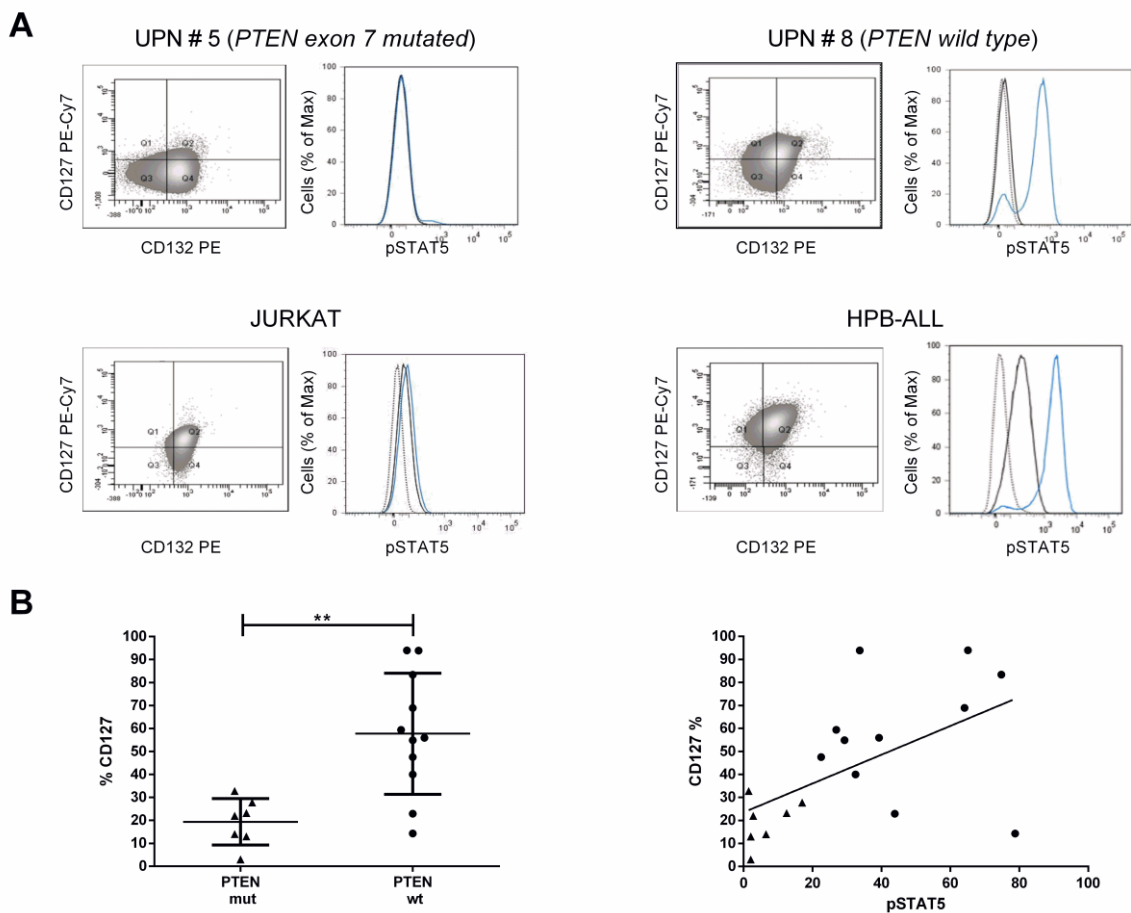
ALL nor in T lymphocytes activation (**Supplementary Figure 5**), might indicating that such pathways not be directly activated by IL7.

Supplementary Figure 5: IL7-induced PI3K signaling response. Basal (black bars) and IL7-induced (grey bars) phosphorylation was also studied for p4EBP1 (panel **A**), pS6 (panel **B**) and pAkt473 (panel **C**). No statistical differences were observed between the two conditions in either PTEN wt or PTEN mutated T-ALL samples nor in residual T cells with concordant data as assessed by MFI values.



In order to investigate the lack of pSTAT5 response in *PTEN* mutated T-ALL cells we measured CD127 and CD132 (both of IL7 receptor components) surface expression in T-ALL blasts from 18 patients (7/18 *PTEN* exon 7 mutated and 11/18 *PTEN* wt). As shown in **Figure Results 15A** we found that the expression of IL7 receptor (IL7 R) proteins was clearly detectable in all *PTEN* exon 7 mutated samples despite they were pSTAT5 non-responsive; however, CD127 was statistically lower as compared to wild type samples (CD127: mean $19.4\pm 3.8\%$ vs $57.7\pm 7.9\%$ $p<0.01$; CD132: mean $46.7\pm 11.7\%$ vs $59.9\pm 8.0\%$). Regarding CD127 expression, we aimed at investigating the correlation between its surface expression and the IL7-induced pSTAT5 response, by a regression plot analysis, and we observed a significant correlation between these parameters ($r^2=0.319$, $p=0.01$, **Figure Results 15B**). Further, we assessed IL7R expression and pSTAT5 response in Jurkat and HPB-ALL cell lines. Jurkat cells expressed both CD127 and CD132 at high levels (65.4% and 84.2% respectively) despite being pSTAT5 non-responsive to IL7. Yet, *PTEN* wt HPB-ALL cells showed a very high IL7R expression (CD127=97.5% and CD132=95.8%), and a strong IL7-induced pSTAT5 response (92.4%).

Figures Results 15: Immunophenotypic expression of the IL7 receptor according to PTEN status and correlation with IL7-induced STAT5 phosphorylation. **Panel A:** representative dual plots of CD127/CD132 phenotypic expression and related histogram of pSTAT5 expression upon IL7 stimulation in representative PTEN exon 7 mutated and wt patients, in Jurkat and HPB-ALL cell lines. In histograms blue line represents IL7-induced pSTAT5 expression, dashed line represents Isotype negative control, gray continuous line represents the basal expression, and the blue line represents the IL7-driven expression. **Panel B:** percentage expression of surface CD127 in 18 primary T-ALL samples and linear correlation between response to IL7 stimulation and IL7 Receptor expression. Pearson coefficient (p) has indicated a moderately positive correlation between the two variables ($p=0.56$). PTEN Exon7 wt and mutated patients are indicated by circles and triangles respectively.



IL7-mediated T-ALL cell survival

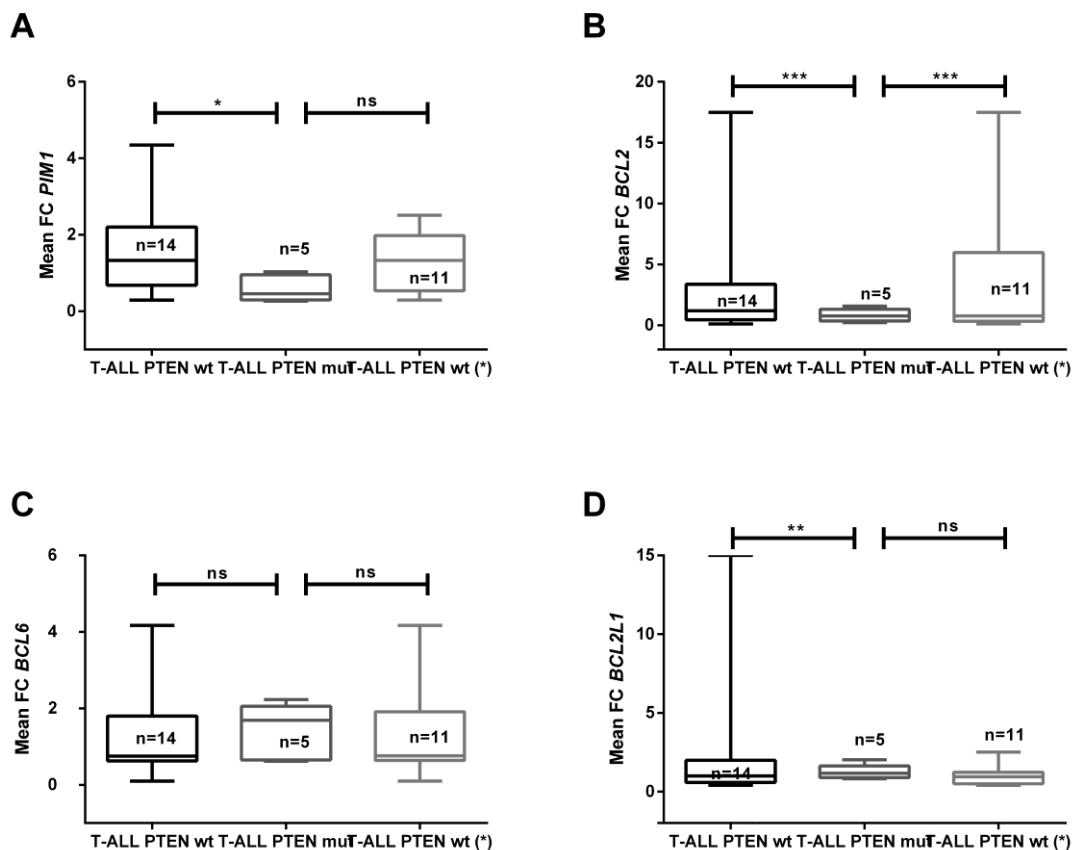
To explore the functional involvement of IL7-mediated cell growth, we cultured 8 primary samples (4 *PTEN* exon 7 mutated and 4 *PTEN* wt) for 72 hours in the presence or absence of IL7. We found that cell survival was not affected in 3 out of 4 mutated samples and Jurkat cells showed similar IL7-independent survival. In *PTEN* wt samples the result was heterogeneous with two samples showing an IL7-induced increased survival and two samples not affected (**Supplementary Materials**).

RT-qPCR analysis of gene transcript levels IL7 regulated in T-ALL patients

To determine the functional role of IL7 in survival, growth and proliferation, we also determined the transcription levels of the following genes *PIM1*, *BCL2*, *BCL6* and *BCL2L1* genes. We studied 19 out of 25 T-ALLs including 5 *PTEN* exon7 mutated patients. We observed a significantly higher *PIM1* expression in *PTEN* exon7 wt patients as compared to the mutated ones ($p=0.032$). When we excluded three patients with *PTEN* exon7 wt and basal pSTAT5 overexpressed (due to mutations in *IL7R α* Exon6 and other rearrangements), *PIM1* loses the statistical significance despite the difference in fold change (1.293 Vs 0.588 respectively) (**Figure Results 16A**). *BCL2* expression was statistically higher in *PTEN* wild-type patients (**Figure Results 16B**), this data support the report by Ribeiro et al. (27) showing that IL7 upregulates *BCL2* via PI3K/Akt pathway, therefore in *PTEN* exon7 mutated T-ALLs STAT5 may induce cell survival by an alternative Bcl-2 independent mechanism. Finally, *BCL6* and *BCL2L1* expression resulted non-statistically significant between the two subgroups ($p>0.05$, **Figures 16C and 16D**). Primer pairs used in RT-qPCR are shown in **Supplementary Table 4**.

Figure Results 16: RT-qPCR analysis of gene transcript levels in T-ALL patients.

Panel A: Box plot representation of PIM1 transcript level in PTEN Exon7 mutated (n=5) and PTEN Exon7 wild type T-ALL with (n=14) or (*) without pSTAT5 basically overexpressed patients (n=11). The difference between the two subgroups became non-statistically significant despite the difference in Fold Change means (1.293 Vs 0.588 respectively) (p>0.05). **Panel B:** BCL2 different expression between PTEN mutated and PTEN wild type T-ALL cases was confirmed despite the exclusion of pSTAT5 basically overexpressed patients (p=0.0005) (*). **Panel C:** BCL6 expression was non-statistically significant between the T-ALL subgroups: one with PTEN mutation, one with PTEN wild-type (p>0.05), and (*) one with PTEN wild-type excluding those with pSTAT5 overexpressed. **Panel D:** Box plot representation of BCL2L1 expression in T-ALL cases. We observed that the different expression was statistically significant comparing PTEN mutated Vs PTEN wild-type T-ALL (p=0.001). When we excluded (*) those patients with pSTAT5 basically overexpressed (due to alterations in IL7R α Exon6 or other rearrangements such as NUP214/ABL1 or ETV6/ABL), this expression difference became non-statistically significant



Supplementary Table 4: Primer pairs used in RT-qPCR

Gene name	Designation	Sequence 5'-3'	Application
<i>BCL2</i>	Forward	ATGTGTGTGGAGAGCGTCAACC	RT-qPCR
	Reverse	TGAGCAGAGTCTTCAGAGACAGCC	
<i>BCL2L1</i> (Bcl-xL)	Forward	GGAACAATGCAGCAGCCGAG	RT-qPCR
	Reverse	GTAGAGTGGATGGTCAGTGT	
<i>BCL6</i>	Forward	GTTGTGGACACTTGCCGGAA	RT-qPCR
	Reverse	CTCTTCACGAGGAGGCTTGAT	
<i>PIM1</i>	Forward	CGAGCATGACGAAGAGATCAT	RT-qPCR
	Reverse	TCGAAGGTTGGCCTATCTGA	

DISCUSSION

Due to high-risk disease characteristics and significant toxicity associated with chemotherapy, ALL outcome is less encouraging for defined subgroups of patients [44]. Novel targeted therapies offer the promise of effective anti-leukemic activity with reduced toxicity but given the different molecular and genetic alterations occurring in ALL, it is improbable that a single agent will be effective for all patients with ALL. For this reason, it becomes needful to identify a patient-specific therapy. Moreover, some subgroup of leukemia such as T-ALL or “B-Others” have no useful markers to assessing the disease follow up and so predictive disease markers should be identified. In order to individuate new markers of disease helping the clinicians to identify new patients-specific therapy, we focused to study three important genes involved in the main metabolic pathways of pediatric ALL. CK2 (Casein Kinase 2) is a regulatory serine/threonine kinase ubiquitously expressed and its activity is required for activation of pro-survival pathways [45]. Several pathways (WNT/ β -Catenin, p53 and PI3K/AKT/PTEN with ERG overexpression) may contribute to the dysregulation of kinase signaling such as Casein Kinase 2 (CK2), which results in resistance to kinase inhibitors. The importance of phosphorylation makes protein kinases and phosphatases promising therapeutic targets for a wide variety of human disorders [46]. Recent research has provided evidence favoring role of CK2 in a multitude of biological processes, its function in regulating cellular growth and proliferation on cancer cells [47]. CK2 overexpression has been confirmed in all hematological malignancies including precursor lymphoid (T- and B-Acute Lymphoblastic Leukemia) [48] and acute myeloid leukemia [49]. Overexpression of CK2 appears to impart a survival advantage in cancer cells by suppressing apoptosis through its action on a variety of cellular and nuclear substrates and favoring cell growth. Transcription factor Ikaros acts as a tumor suppressor in T-cell acute lymphoblastic leukemia (T-ALL) and B-ALL [32]. IKZF1 haploinsufficiency is sufficient to result in malignant transformation and the development of

acute lymphoblastic leukemia [50]; genome-wide analysis have shown that 30% of pediatric B-ALL and approximately 5% of T-ALL involve deletion or dysfunction of the IKZF1 gene. Ikaros, like many other proteins, undergoes posttranslational modifications such as phosphorylation. Ikaros is a direct substrate of CK2 in hematopoietic cells: CK2 phosphorylates Ikaros and impairs Ikaros function as a tumor suppressor in leukemia model. Molecular and pharmacological inhibition of CK2 was shown to restore Ikaros' function as a tumor suppressor. Recent studies have shown that CX-4945, small molecule orally bioavailable, exerts its anti-leukemic effect via inhibition of CK2-mediated phosphorylation. This supports the use of CX-4945 in a phase I clinical trial for treatment of high-risk relapsed hematologic malignancies [51]. Recent studies indicated that in adult lymphoblastic leukemia patients, high c-MYC expression correlates with clinical high-risk factors and high proliferation markers. Moreover, c-MYC is a Ikaros target gene [52] and so CK2 inhibitor acts as an Ikaros activator and suppresses c-MYC expression in an Ikaros-dependent manner in ALL cells. The Ets-related gene ERG (erythroblastosis virus E26 transforming sequence family member) is involved in signal transduction pathways that regulate and promote cell differentiation, proliferation and tissue invasion [39]. ERG is preferentially and strongly expressed in the immature B- and T-lymphoid lineages, in addition to myeloid lineage cells. Previous studies suggest that ERG overexpression is associated with inferior clinical outcome [37]. In T-ALL patients, a high level of ERG expression has been associated with poor relapse-free survival [38]. Recent studies reported that, due to enrichment of the PI3K/AKT signaling cascade, ERG overexpression induces resistance to kinase inhibitors including Sorafenib and TKI258 (Dovitinib) [7]. A recent study also demonstrated that co-activation of the PI3K/AKT pathway and ERG overexpression collaborate with lack of PTEN and prostate specific androgen response (AR) in the development of prostate carcinoma [53]. Functional assays revealed that ERG may modulate kinase signaling pathways but there is no data that shows the direct correlation between CK2 and Erg expression. ERG overexpression resulted in dephosphorylation AKT(Ser473) suggesting that ERG overexpression

represses AKT activation. Thus, *ERG* overexpression leads one to believe that alternate signaling pathways are responsible for *ERG* mediated kinase resistance in leukemia. So, Bock J, Baldus et al. proposed that *ERG* driven drug resistance overrides PI3K/AKT signaling by alternate pathways. These alternative pathways need to be further investigated for effective drug design and adapted therapies for *ERG* overexpressing high-risk leukemias [7].

The expression of *CK2* in association with *MYC* and *ERG* overexpression has not been characterized in biological subgroups of pediatric ALL, yet. The characterization of these genes would integrate new markers of disease and/or therapeutic targets in pediatric ALL.

Here we demonstrated that *CK2* is overexpressed in pediatric ALL. Both T- and B-ALLs show higher level of *CK2* expression comparing with HDs. Moreover, in T-ALLs with HR features we showed a median *CK2* expression up to 5 times higher than HDs. *IKZF1*, a prognostic factor in pediatric ALL, is deleted either in children with T-ALL (3 out of 20 cases), showing a high expression of *ERG* and *CK2*, which continues to be confirmed as future therapeutic targets. We also showed, for the first time, a correlation between *MYC* overexpression, *TLX3 (HOX11L2)* rearrangement and *CRLF2* overexpression in T-ALL. *MYC-high* expression was seen in seven *TLX3 (HOX11L2)* rearranged (7 out of eight non-HR T-ALL patients), generally correlated with a poor prognosis [54]. Moreover, five out of 7 non-HR T-ALLs showed a *CRLF2* overexpression, which has recently demonstrated a poor prognostic marker in children with T-ALL [55]. These findings confirmed that *TLX3* expression is not a prognostic indicator in pediatric T-ALL [56] and that high levels of *MYC* expression are broadly present in T-ALL [57]. In patients with *PTEN-Exon7* mutation, as expected, we observed a low expression of *MYC*. Conversely, we showed that in pediatric B-ALLs is evident a correlation between a *MYC-high* profile and poor prognostic genetic subgroups. Interestingly, patients with an 11q23-R or *MLL*-rearranged B-ALL show an extremely high level of *MYC* expression. Accordingly, it has been recently shown that the proliferation of *MLL*-rearranged B-ALL cells was decreased upon *MYC* depletion and that *MYC*-

protein abundance in *MLL*-rearranged B-ALL cells was much higher than in non-*MLL*-rearranged B-ALL cells [58]. The oncogenic potential of the transcription factor *ERG* induced us to determine the prognostic impact of *ERG* in pediatric ALL. Our data hint an *ERG* overexpression in pediatric ALL comparing with HDs, particularly we identified high *ERG* expression as an independent adverse prognostic factor in children with high risk T-ALL with an expected inferior outcome. Based on our data, we outlined a patient-specific profile based on the expression of these three biomarkers (*CK2*, *MYC*, *ERG*) and the mutational screening for *PTEN-Exon7*, *IKZF1* and *TLX3* gene. The *CK2* overexpression associated with *ERG* overexpression (independently from *MYC* expression) related to other genetic alterations (*PTEN Exon7* mutation, *CDKN2A* or *IKZF1* deletion) could be helpful in the identification of a patient-specific profile. We could speculate a “*IKZF1-plus* group” for T-ALL: *CK2-high*, *ERG-high*, *PTEN Exon7* mutation, *CDKN2A* and *IKZF1* deletion identify a subgroup of pediatric T-ALL patients with a very poor outcome (Relapse, DOC, Dead for progressive disease). Despite the several molecular events that drive the different human leukemia subtypes, high *CK2* levels appeared as a common denominator in all of them, suggesting that *CK2* targeting could represent a multi-potential therapeutic strategy [59]. New relevant molecular markers can guide risk-adapted treatment strategies and will be the basis for the development of new targeted therapies. Our findings strongly suggest that *CK2* and *ERG* could be those targets.

About signaling network involved in pediatric T-ALL, Previous reports demonstrated a cross-talk between *IL7R* signaling pathway and *PI3K* that ultimately leads to either *STAT5* or *Akt* activation [23]. Yet, stimulation by *IL7* triggers the phosphorylation of various pathways such as *JAK/STAT*, *Ras/MAPK* and *PI3K* [60]. To better understand the role of these signaling pathways in *PTEN* mutated pediatric T-ALL, we first sought to establish the expression levels of the various *PI3K* and *JAK/STAT* downstream effectors using phosphoflow analysis [41]. In our hands phosphoflow and WB approaches provided consistent results throughout different sets of experiments. Yet,

phosphoflow analysis can be performed in around three hours from sample collection or thawing. Reproducibility was high as demonstrated by the consistent signaling profile of normal T lymphocytes detected in healthy Hasegawa bone marrow samples and in T-ALL samples. Notably this approach can allow to analyze signaling pathways in heterogeneous populations by appropriated gating strategies. In this regard we were able to dissect different signaling pathways in two different PTEN subclones of the same T-ALL sample (data not shown, manuscript in preparation). Then we studied PI3K/Akt pathway in three T-ALL cell lines bearing different *PTEN* status, and we found constitutive hyperactivation of PI3K/Akt pathway in all tested cells confirming previous data [12]. PTEN protein resulted not expressed neither in CEM nor in JURKAT cells (both *PTEN* mutated), whereas it was expressed in the *PTEN* wild type HPB-ALL cells. By contrast not constitutive phosphorylation of STAT5 or STAT3 was observed in CEM and Jurkat cells (both *PTEN* mutated), with only partial pSTAT5 expression in HPB-ALL cells. Phosphoflow-based pSTATs measurement has been previously validated in our hands although in different cellular subsets [61].

We then determined the activation status of p4EBP1, PTEN, pAkt S473 and pS6 in primary T-ALL cells as compared to T cells from normal BM samples. Patient's samples showed higher protein levels confirming the constitutive hyperactivation of PI3K pathway in T-ALL [21]. Surprisingly when we separated our T-ALL cohort based on *PTEN* status, we observed a higher pAkt S473 activation and a lower pS6 and 4pEBP1 activation in PTEN mutated samples as compared to the wt samples. In order to assess the accuracy of our phosphoflow approach in measuring modulated phospho-signaling nodes, we tested specific inhibitors and stimuli. We confirmed that NVP-BEZ235 is able to decrease not only Akt 473 phosphorylation but also some mTOR downstream targets such as p4EBP1 and pS6 in both primary T-ALL and T-ALL cell lines. These results suggest that sensitivity of T-ALL to PI3K inhibition is determined by activation of the PI3K/Akt

pathway rather than the level of PTEN expression, and confirm the utility of assessing the phosphorylation *status* of Akt, S6 and 4EBP1 as biomarkers for responsiveness among different leukemic subtypes [21,40-44].

We next investigated the JAK/STAT5 pathway by measuring basal and IL7-induced pSTAT5 levels. We showed that T-ALL blasts were not constitutively activated, with the exception of three patients [two carrying translocations involving ABL1 gene and one with IL7R α (Exon6) mutation] and the HPB-ALL cell line, which expresses endogenous pSTAT5. Intriguingly, we observed IL7-induced strong pSTAT5 responsiveness only in *PTEN* exon 7 wt blasts (11 out of 11 T-ALL primary samples) whereas mutated blasts were highly refractory to IL7 action. Similarly, HPB-ALL *PTEN* wt cells were highly pSTAT5-responsive to IL7, while *PTEN* exon 7 deleted/mutated cell lines were completely non-responsive. Liu et al [62] performed an integrated genomic analysis in childhood and young adult T-ALL to identify the spectrum and constellations of genetic alterations in this disease and identify 10 recurrently altered pathways. For example, they found that JAK3/STAT5B mutations are exclusively segregated in HOX1 deregulated ALL while PIK3R1/PTEN mutations are in TAL1 ALL, suggesting that different signaling pathways have distinct roles according to maturational stage. However, around 20% of cases had multiple signaling mutations (i.e. JAK-STAT activating mutation and concomitant PI3K-AKT mutations) raising the question of existing multiclonal and/or sub-clones. In our study only 2 out of 7 *PTEN* Exon7 mutated T-ALL were TAL1 mutated and also maturation stage did not segregate significantly among the two subgroups (Supplementary Table 1). Although in a limited series of patients, our study here demonstrated that *PTEN* Exon7 T-ALL are distinctly responsive to IL7 *in vitro* corroborating genetic landscape data.

IL7 is a pro-survival factor present in plasma and in lymphopoietic niches that protects T-cells and T-ALL cells from spontaneous [63] and chemotherapy-induced apoptosis [64].

TAL1 is a basic helix–loop– helix transcription factor and ectopically expressed in 20–30% of T-ALL patients either via chromosomal rearrangements or by upstream somatic mutations leading to the generation of a super-enhancer and that there is a close association between TAL1 expression and *PTEN* deletion [65]. Bornschein and collaborators [65] in an *ex-vivo* pro-T cell culture model showed that both TAL1+ pro-T cells and TAL1+ T-ALL cells were unable to induce STAT5 phosphorylation *in vitro* upon IL7 stimulation. They found that *PTEN* deleted/TAL1+ pro-T cells could grow in the absence of IL7, in contrast to *PTEN* deleted alone cells. We observed that only 2 out of 7 *PTEN* mutated T-ALL cases (supplementary Table 1) was TAL1+, suggesting that *PTEN* deletion in T-ALL can be *per se* a driver event in repressing IL7-mediated signaling.

We then investigated the correlation between IL7-driven pSTAT5 response and the expression of CD127 surface molecule in eighteen T-ALL samples according to *PTEN status*. Although the expression of CD127 was significantly higher in *PTEN* wt vs *PTEN* mutated samples, pSTAT5 response resulted only partially dependent on the amount of IL7 receptor. Furthermore, *PTEN* exon 7 mutated Jurkat cell line with high expression of IL7R molecules was completely non-responsive to IL7. Recently, Ribeiro et al. [27] demonstrated that signaling via STAT5 is mandatory for IL7-mediated survival, proliferation and growth of T-ALL cells and it is required for increasing cell viability and cell cycle progression induced by IL7. However, IL7-mediated upregulation of BCL2 in T-ALL is independent of STAT5 activity. Thus, we investigated BCL2 expression in *PTEN* Exon7 wt and mutated patients, respectively, and we observed a BCL2 downregulation in *PTEN* Exon7 mutated T-ALLs confirming findings reported by Ribeiro et al. Another IL7 and STAT5 target is PIM1 which can be upregulated by both IL7 and STAT5. We then could speculate that an alternative IL7/IL7R signaling responsible for the leukemogenic activity could be active in *PTEN* Exon7 mutated T-ALL patients [66].

In summary, we demonstrated that phosphoflow analysis represents a fast, reliable and accurate approach to assess the signaling profiling of T-ALL, including *in vitro* testing of either traditional drugs or novel small molecule inhibitors over the traditional biochemical methods such as WB [67, 68]. In this context we also validated the use of residual normal T cells as a valuable internal control. Yet our results show that *PTEN* mutated T-ALLs do not activate STAT5 and consequently they might not use this IL7R-driven pathway to promote survival and proliferation. According to this view we found significantly lower expression of downstream gene *BCL2* in *PTEN* mutated T-ALLs. It possible that these cells activate PI3K/Akt signaling constitutively to a higher degree than *PTEN* wt as indicated by the higher level of Akt phosphorylation, however further investigations are necessary to elucidate the significance of this peculiar signaling profile of *PTEN* mutated T-ALL. We believe that our observations should be taken into account in future studies aiming at molecular targeting of PI3K and/or JAK/STAT pathways for pharmacological intervention in T-ALL.

REFERENCES

1. Pui CH, Carroll WL, Meshinchi S, Arceci RJ. Biology, risk stratification, and therapy of pediatric acute leukemias: an update. *J Clin Oncol.* 2011, 29(5):551-65. Erratum in: *J Clin Oncol.* 2011, 29(36):4847
2. Tasian SK, Loh ML, Hunger SP. Childhood acute lymphoblastic leukemia: Integrating genomics into therapy. *Cancer.* 2015, 121(20):3577-
3. Jennifer S Woo, Michael O Alberti and Carlos A Tirado. Childhood B-acute leukemia: a genetic update. *Exp Hematol Oncol.* 2014,3:16. Review.
4. Terwilliger T, Abdul-Hay M. Acute lymphoblastic leukemia: a comprehensive review and 2017 update. *Blood Cancer J.* 2017, 7(6):e577. Review
5. Schrappe M, Valsecchi MG, Bartram CR, Schrauder A, Panzer-Grümayer R, Möricke A, Parasole R, Zimmermann M, Dworzak M, Buldini B, Reiter A, Basso G, Klingebiel T, Messina C, Ratei R, Cazzaniga G, Koehler R, Locatelli F, Schäfer BW, Aricò M, Welte K, van Dongen JJ, Gadner H, Biondi A, Conter V. Late MRD response determines relapse risk overall and in subsets of childhood T-cell ALL: results of the AIEOP-BFM-ALL 2000 study. *Blood.* 2011, 118(8):2077-84. doi: 10.1182/blood-2011-03-338707.
6. JA McCubrey, LS Steelman, WH Chappell, SL Abrams, RA Franklin, G Montalto, M Cervello, M Libra, S Candido, G Malaponte, MC Mazzarino, P Fagone, F Nicoletti, J Basecke, S Mijatovic, D Maksimovic-Ivanic, M Milella, A Tafuri, F Chiarini, C Evangelisti, L Cocco and AM Martelli. Ras/Raf/MEK/ERK and PI3K/PTEN/Akt/mTOR Cascade Inhibitors: How Mutations Can Results in Therapy Resistance and How to Overcome Resistance. *Oncotarget.* 2012, 3(10): 1068-1111
7. Bock J, Mochmann LH, Schlee C, Farhadi-Sartangi N, Göllner S, Müller-Tidow C, Baldus CD. ERG transcriptional networks in primary acute leukemia cells implicate a role for ERG in deregulated kinase signaling. *PLoSOne.* 2013, 8(1):e52872. doi: 10.1371/journal.pone.0052872.
8. Okkenhaug K, Vanhaesebroeck B. PI3K in lymphocyte development, differentiation and activation. *Nat. Rev. Immunol.* 2003;3:317–330.
9. Milella M, Falcone I, Conciatori F, Cesta Incani U, Del Curatolo A, Inzerilli N, Nuzzo CMA, Vaccaro V, Vari S, Cognetti F, Ciuffreda L. PTEN: Multiple Functions in Human Malignant Tumors. *Front. Oncol.* 2015;5:24.
10. Mendes RD, Cante-Barrett K, Pieters R, Meijerink JPP. The relevance of PTEN-AKT in relation to NOTCH1-directed treatment strategies in T-cell acute lymphoblastic leukemia. *Haematologica* 2016;101:1010–1017.

11. Sakai A, Thieblemont C, Wellmann A, Jaffe ES, Raffeld M. PTEN gene alterations in lymphoid neoplasms. *Blood* 1998;92:3410–3415.
12. Shan X, Czar MJ, Bunnell SC, Liu P, Liu Y, Schwartzberg PL, Wange RL. Deficiency of PTEN in Jurkat T cells causes constitutive localization of Itk to the plasma membrane and hyperresponsiveness to CD3 stimulation. *Mol. Cell. Biol.* 2000;20:6945–6957.
13. Oliveira ML, Akkapeddi P, Alcobia I, Almeida AR, Cardoso BA, Fragoso R, Serafim TL, Barata JT. From the outside, from within: Biological and therapeutic relevance of signal transduction in T-cell acute lymphoblastic leukemia. *Cell. Signal.* 2017;38:10–25.
14. Sansal I, Sellers WR. The biology and clinical relevance of the PTEN tumor suppressor pathway. *J. Clin. Oncol.* 2004;22:2954–2963.
15. Georgescu MM, Kirsch KH, Akagi T, Shishido T, Hanafusa H. The tumor-suppressor activity of PTEN is regulated by its carboxyl-terminal region. *Proc. Natl. Acad. Sci. U. S. A.* 1999;96:10182–10187.
16. Zuurbier L, Petricoin EF 3rd, Vuerhard MJ, Calvert V, Kooi C, Buijs-Gladdines JGCAM, Smits WK, Sonneveld E, Veerman AJP, Kamps WA, Horstmann M, Pieters R, Meijerink JPP. The significance of PTEN and AKT aberrations in pediatric T-cell acute lymphoblastic leukemia. *Haematologica* 2012;97:1405–1413.
17. Jotta PY, Ganazza MA, Silva A, Viana MB, da Silva MJ, Zambaldi LJG, Barata JT, Brandalise SR, Yunes JA. Negative prognostic impact of PTEN mutation in pediatric T-cell acute lymphoblastic leukemia. *Leukemia* 2010;24:239–242.
18. Jenkinson S, Kirkwood AA, Goulden N, Vora A, Linch DC, Gale RE. Impact of PTEN abnormalities on outcome in pediatric patients with T-cell acute lymphoblastic leukemia treated on the MRC UKALL2003 trial. *Leukemia* 2016;30:39–47.
19. Paganin M, Grillo MF, Silvestri D, Scapinello G, Buldini B, Cazzaniga G, Biondi A, Valsecchi MG, Conter V, Te Kronnie G, Basso G. The presence of mutated and deleted PTEN is associated with an increased risk of relapse in childhood T cell acute lymphoblastic leukaemia treated with AIEOP-BFM ALL protocols. *Br. J. Haematol.* 2018;182:705–711.
20. Palomero T, Sulis ML, Cortina M, Real PJ, Barnes K, Ciofani M, Caparros E, Buteau J, Brown K, Perkins SL, Bhagat G, Agarwal AM, Basso G, Castillo M, Nagase S, Cordon-Cardo C, Parsons R, Zuniga-Pflucker JC, Dominguez M, Ferrando AA. Mutational loss of PTEN induces resistance to NOTCH1 inhibition in T-cell leukemia. *Nat. Med.* 2007;13:1203–1210.
21. Silva A, Yunes JA, Cardoso BA, Martins LR, Jotta PY, Abecasis M, Nowill AE, Leslie NR, Cardoso AA, Barata JT. PTEN posttranslational inactivation and hyperactivation of the PI3K/Akt pathway sustain primary T cell leukemia viability. *J. Clin. Invest.* 2008;118:3762–3774.

22. Gutierrez A, Sanda T, Grebliunaite R, Carracedo A, Salmena L, Ahn Y, Dahlberg S, Neuberg D, Moreau LA, Winter SS, Larson R, Zhang J, Protopopov A, Chin L, Pandolfi PP, Silverman LB, Hunger SP, Sallan SE, Look AT. High frequency of PTEN, PI3K, and AKT abnormalities in T-cell acute lymphoblastic leukemia. *Blood* 2009;114:647–650.
23. Barata JT, Silva A, Brandao JG, Nadler LM, Cardoso AA, Boussiotis VA. Activation of PI3K is indispensable for interleukin 7-mediated viability, proliferation, glucose use, and growth of T cell acute lymphoblastic leukemia cells. *J. Exp. Med.* 2004;200:659–669.
24. Johnson SE, Shah N, Bajer AA, LeBien TW. IL-7 Activates the Phosphatidylinositol 3-Kinase/AKT Pathway in Normal Human Thymocytes but Not Normal Human B Cell Precursors. *J. Immunol.* 2008;180:8109–8117.
25. Silva A, Laranjeira ABA, Martins LR, Cardoso BA, Demengeot J, Yunes JA, Seddon B, Barata JT. IL-7 contributes to the progression of human T-cell acute lymphoblastic leukemias. *Cancer Res.* 2011;71:4780–4789.
26. Jiang Q, Li WQ, Aiello FB, Mazzucchelli R, Asefa B, Khaled AR, Durum SK. Cell biology of IL-7, a key lymphotrophin. *Cytokine Growth Factor Rev.* 2005;16:513–533.
27. Ribeiro D, Melao A, van Boxtel R, Santos CI, Silva A, Silva MC, Cardoso BA, Coffey PJ, Barata JT. STAT5 is essential for IL-7-mediated viability, growth, and proliferation of T-cell acute lymphoblastic leukemia cells. *Blood Adv.* 2018;2:2199–2213.
28. Rich BE, Campos-Torres J, Tepper RI, Moreadith RW, Leder P. Cutaneous lymphoproliferation and lymphomas in interleukin 7 transgenic mice. *J. Exp. Med.* 1993;177:305–316.
29. Abraham N, Ma MC, Snow JW, Miners MJ, Herndier BG, Goldsmith MA. Haploinsufficiency identifies STAT5 as a modifier of IL-7-induced lymphomas. *Oncogene* 2005;24:5252–5257.
30. Dibirdik I, Langlie MC, Ledbetter JA, Tuel-Ahlgren L, Obuz V, Waddick KG, Gajl-Peczalska K, Schieven GL, Uckun FM. Engagement of interleukin-7 receptor stimulates tyrosine phosphorylation, phosphoinositide turnover, and clonal proliferation of human T-lineage acute lymphoblastic leukemia cells. *Blood* 1991;78:564–570.
31. Melao A, Girio A, Barata JT. CK2 Basal Activity Regulates IL-7 Mediates JAK/STAT and PI3K/Akt Pathway Activation and Pro-Survival effects in T-Cell Acute Lymphoblastic Leukemia Cells. *Blood* 2012, 1242
32. Mullighan CG, Miller CB, Downing JR et al. BCR-ABL1 lymphoblastic leukemia is characterized by the deletion of Ikaros. *Nature*, 2008 May1;453(7191):110-4
33. Philippe Kastner and Susan Chan, Role of IKZF1 in T-cell acute lymphoblastic leukemia. *World Journal of Biological Chemistry*, 2011 June. 2(6): 108-114
34. De Barrios O, Meler A and Parra M. MYC's Fine Line Between B Cell Development and Malignancy. *Cells*, 2020 Feb. doi: 10.3390/cells9020523

35. Kaur M, Cole MD. MYC acts via the PTEN tumor suppressor to elicit autoregulation and genome-wide gene repression by activation of the Ezh2 methyltransferase. *Cancer Res.* 2013, 73(2):695-705
36. Channavajhala P, Seldin DC. Functional interaction of protein kinase CK2 and c-Myc in lymphomagenesis. *Oncogene.* 2002, 21(34):5280-8
37. Marcucci G, Baldus CD et al. Overexpression of the ETS-related gene, ERG, predicts a worse outcome in acute myeloid leukemia with normal karyotype: A Cancer and Leukemia Group B study. *J Clin Oncol.* 2005. 23:9234-9242.
38. Baldus CD, Burmeister T, Martus P, Schwartz S, Gökbuget N, Bloomfield CD, Hoelzer D, Thiel E, Hofmann WK. High expression of the ETS transcription factor ERG predicts adverse outcome in acute T-lymphoblastic leukemia in adults. *J Clin Oncol.* 2006, 24(29):4714-4720
39. Zhao HZ, Jia M, Luo ZB, Xu XJ, Li SS, Zhang JY, Guo XP, Tang YM. ETS-related gene is a novel prognostic factor in childhood acute lymphoblastic leukemia. *Oncol Lett.* 2017, 13(1):455-462.
40. Tazzari PL, Cappellini A, Bortul R, Ricci F, Billi AM, Tabellini G, Conte R, Martelli AM. Flow cytometric detection of total and serine 473 phosphorylated Akt. *J. Cell. Biochem.* 2002;86:704–715.
41. Krutzik PO, Irish JM, Nolan GP, Perez OD. Analysis of protein phosphorylation and cellular signaling events by flow cytometry: techniques and clinical applications. *Clin. Immunol.* 2004;110:206–221.
42. Pongers-Willems MJ, Seriu T, Stolz F, D’Aniello E, Gameiro P, Pisa P, Gonzalez M, Bartram CR, Panzer-Grümayer ER, Biondi A, San Miguel JF, Van Dongen JJM. Primers and protocols for standardized detection of minimal residual disease in acute lymphoblastic leukemia using immunoglobulin and T cell receptor gene rearrangements and TAL1 deletions as PCR targets. Report of the BIOMED-1 CONCERTED ACTION: Investiga. *Leukemia* 1999;13:110–118.
43. Brian J. Altman, Chi V. Dang. Normal and cancer cell metabolism: lymphocytes and lymphoma. *The FEBS Journal.* 2012
44. D Bhojwani, SC Howard, CH Pui. High-Risk Childhood Acute Lymphoblastic Leukemia. *Clin Lymphoma Myeloma.* 2009, 9 Suppl 3: S222-30
45. Ribeiro ST, Tesio M, Ribot JC, Macintyre E, Barata JT, Silva-Santos B. Casein kinase 2 controls the survival of normal thymic and leukemic $\gamma\delta$ T cells via promotion of AKT signaling. *Leukemia.* 2017, 31(7):1603-1610
46. Cohen P. Protein kinases the major drug targets of the twenty-first century? *Nat Rev Drug Discov.* 2002, 1(4):309-15

47. Gowda C, Dovat S et al. Casein Kinase II (CK2) as a therapeutic target for hematological malignancies. *Curr Pharm Design*, 2017; 23(1):95-107
48. Martins LR, BarataJT et al. Targeting CK2 overexpression and hyperactivation as a novel therapeutic tool in chronic lymphocytic leukemia. *Blood*, 2010; 116:2724-31
49. Kim JS, Min YH et al. Protein kinase CK2 α as an unfavorable prognostic marker and novel therapeutic target in acute myeloid leukemia. *Clin Canc research*, 2007; 13:1019-28
50. Davis KL. Ikaros: master of hematopoiesis, agent of leukemia. *Ther Adv hematol*, 2011; 2:359-68
51. Song C, Gowda C, Dovat S et al. Targeting casein kinase II restores Ikaros tumor suppressor activity and demonstrates therapeutic efficacy in high-risk leukemia. *Blood*. 2015, 126(15):1813-22
52. Ge Z, Dovat S, Song C et al. Clinical significance of high c_Myc and low MYCBP2 expression and their association with Ikaros dysfunction in adult acute lymphoblastic leukemia. *Oncotarget*, 2015; 6: 42300-11
53. Carver BS, Tran J, Gopalan A et al. 2009, Aberrant ErG expression cooperates with loss of PTEN to promote cancer progression in the prostate. *Nature Genetics* 41(5): 619-624
54. Attarbaschi A, Pisecker M, Inthal A, Mann G, Janousek D, Dworzak M, Potechner U, Ullmann M, Schrappe H, Gadner OA, Haas R, Panzer-Grumayer S, Strehl S, on behalf of the Austrian Berlin-Frankfurt-Munster (BFM) Study Group. Prognostic relevance of TLX3 (HOX11L2) expression in childhood T-cell acute lymphoblastic leukaemia treated with Berlin-Frankfurt-Munster (BFM) Protocols containing early and late re-intensification elements. *British Journal of Haematology*. 2010, 148(2): 293-300
55. Palmi C, Savino AM, Silvestri D, et al. CRLF2 over-expression is a poor prognostic marker in children with high-risk T-cell acute lymphoblastic leukemia. *Oncotarget*. 2016, vol 7, n 37: 59260-59272
56. Ma J, Hua J, Sha Y, Xie Y. The effect of TLX3 expression on the prognosis of pediatric T cell acute lymphocytic leukemia- a systematic review. *Tumour Biol*. 2014, 35(9):8439-43

57. M Sanchez-Martin and A Ferrando. The NOTCH1-MYC highway toward T-cell acute lymphoblastic leukemia. *Blood*. 2017, 129(9): 1124-1133
58. Zhu S, Cheng X, Wang R, Tan Y, Ge M, Li D, Xu Q, Sun Y, Zhao C, Chen S, Liu H. Restoration of MicroRNA function impairs MYC-dependent maintenance of MLL leukemia. *Leukemia*. 2020,34(9):2484-2488
59. Buontempo F, McCubrey JA, Orsini E, Ruzzene M, Cappellini A, Lonetti A, Evangelisti C, Chiarini F, Evangelisti C, Barata JT, Martelli AM. Therapeutic targeting of CK2 in acute and chronic leukemias. *Leukemia*. 2018, 32(1):1-10
60. Carrette F, Surh CD. IL-7 signaling and CD127 receptor regulation in the control of T cell homeostasis. *Semin. Immunol*. 2012;24:209–217.
61. Cazzaniga V, Bugarin C, Bardini M, Giordan M, te Kronnie G, Basso G, Biondi A, Fazio G, Cazzaniga G. LCK over-expression drives STAT5 oncogenic signaling in PAX5 translocated BCP-ALL patients. *Oncotarget* 2015;6:1569–1581.
62. Liu Y, Easton J, Shao Y, Maciaszek J, Wang Z, Wilkinson MR, McCastlain K, Edmonson M, Pounds SB, Shi L, Zhou X, Ma X, Sioson E, Li Y, Rusch M, Gupta P, Pei D, Cheng C, Smith MA, Auvil JG, Gerhard DS, Relling M V, Winick NJ, Carroll AJ, Heerema NA, Raetz E, Devidas M, Willman CL, Harvey RC, Carroll WL, Dunsmore KP, Winter SS, Wood BL, Sorrentino BP, Downing JR, Loh ML, Hunger SP, Zhang J, Mullighan CG. The genomic landscape of pediatric and young adult T-lineage acute lymphoblastic leukemia. *Nat. Genet*. 2017;49:1211–1218.
63. Barata JT, Cardoso AA, Boussiotis VA. Interleukin-7 in T-cell acute lymphoblastic leukemia: an extrinsic factor supporting leukemogenesis? *Leuk. Lymphoma* 2005;46:483–495
64. Wuchter C, Ruppert V, Schrappe M, Dorken B, Ludwig W-D, Karawajew L. In vitro susceptibility to dexamethasone- and doxorubicin-induced apoptotic cell death in context of maturation stage, responsiveness to interleukin 7, and early cytoreduction in vivo in childhood T-cell acute lymphoblastic leukemia. *Blood* 2002;99:4109–4115
65. Bornschein S, Demeyer S, Stirparo R, Gielen O, Vicente C, Geerdens E, Ghesquière B, Aerts S, Cools J, De Bock CE. Defining the molecular basis of oncogenic cooperation between TAL1

expression and Pten deletion in T-ALL using a novel pro-T-cell model system. *Leukemia* 2018;32:941–951.

66. Oliveira ML, Akkapeddi P, Ribeiro D, Melao A, Barata JT. IL-7R-mediated signaling in T-cell acute lymphoblastic leukemia: An update. *Adv. Biol. Regul.* 2019;71:88–96.
67. Hall CP, Reynolds CP, Kang MH. Modulation of Glucocorticoid Resistance in Pediatric T-cell Acute Lymphoblastic Leukemia by Increasing BIM Expression with the PI3K/mTOR Inhibitor BEZ235. *Clin. Cancer Res.* 2016;22:621–632.
68. Evangelisti C, Chiarini F, McCubrey JA, Martelli AM. Therapeutic Targeting of mTOR in T-Cell Acute Lymphoblastic Leukemia: An Update. *Int. J. Mol. Sci.* 2018;19:pii: E1878. doi: 10.3390/ijms19071878.

SUPPLEMENTARY MATERIALS

Cell lines and human normal bone marrows

CCRF-CEM (T-ALL cell line bearing PTEN deletion and CDKN2A deletion), JURKAT (T-ALL cell line bearing PTEN missense mutation, CDKN2A and CREBBP deletion) and REH (B-Cell Precursor ALL cell line bearing ETV6/RUNX1 translocation) were cultured in RPMI-1640 medium with 10% heat-inactivated fetal bovine serum, 1% L-glutamine and 1% Pen-Strep; MHH-CALL-4 (B-ALL cell line bearing JAK2 I682F mutation, constitutive phosphorylation of JAK2 and STAT5 and CRLF2 overexpression) were cultured in RPMI-1640 medium with 20% heat-inactivated fetal bovine serum, 1% L-glutamine and 1% Pen-Strep. Cells were kept at 37° C in 5% CO₂ and splitted out every 3 days.

Validation of *CK2*, *MYC* and *ERG* expression in thymocytes

Thymocytes were also analyzed as normal internal control about *CK2*, *MYC* and *ERG* expression respect to Healthy Donors. *Ck2* expression was absolutely comparable between thymocytes and HDs. Instead, thymocytes FC *Myc* expression was comparable to T-ALL mean FC *MYC* expression. Altman and Dang (FEBS J,2012) have revealed overlapping metabolic rewiring in activated T-cells and *Myc*-transformed lymphocytes due to a series of stimuli (such as IL-7 or IL-2) that support metabolic pathways similar to what happens in tumor cells (with the activation of proto-oncogenes such as c-*Myc*). *Myc* expression is attenuated in normal lymphocytes that return to the basal state, but *Myc*-transformed lymphocytes persistently express *Myc*, which activates genes involved in glucose and glutamine metabolism. *Erg* expression was comparable in thymocytes and HDs too.

RNA isolation and RT-qPCR

Mononuclear cells from BM samples were isolated by Ficoll gradient centrifugation and cryopreserved. Total RNA was extracted using TRizol Reagent (Invitrogen, CA, USA) following the manufacturer's protocols. First strand cDNA was synthesized from total RNA with reverse transcriptase and random primers, using the Superscript Reverse Transcriptase (Invitrogen, CA, USA). Samples were selected based on the quality and quantity of RNA (OD₂₆₀/OD₂₈₀ ratio: 1.8-2.0). Quantitative Real-Time RQ-PCR was performed with a 96-well optic plate using the QuantStudio 7 Flex (Applied Biosystem, Life Technologies). Every sample was tested in duplicate. Expression levels were normalized by *GUS* (endogenous control) and calculated by using the comparative $2^{-\Delta\Delta C_t}$ method. The Comparative cycle Threshold (CT) method was used to determine the relative expression levels of *CK2*, *c-MYC* and *ERG*, using the median of ΔC_t from Healthy controls two replicates and expressed as $2^{-\Delta\Delta C_t}$ ($\Delta C_t = GUS - \text{gene of interest}$). Each reaction mixture consisted of 1 μ l of cDNA, 7.5 μ l of SYBR Green Master Mix, 1 μ l of each primer (250 nmol/ml) and 4.5 μ l of deionized water.

The PCR cycle started with an initial 95°C, 10 minutes melt step, followed by 40 cycles of 15 seconds at 95°C and 60 seconds at 60°C.

In addition, T-ALL patients were screened for the following molecular alterations: *PTEN-Exon7* mutations; *CALM-AF10* transcript; *TP53* and *pS6* mutations; *TXL3* rearrangements and *CRLF2* overexpression, respectively. Primer sequences used for PCR and qRT-PCR in this study are shown in the table below.

All PCR products were size-fractionated by electrophoresis on a 1.5% agarose gel and stained with ethidium bromide using Gel Doc.

Gene target	Primer sequence (5'-3')	Expected amplicons size
CK2 α F	TCATGAGCACAGAAAGCTACGA	158 bp
CK2 α R	AATGGCTCCTTCCGAAAGATC	
c-MYC F	CACCAGCAGCAGCGACTCTGA	63 bp
c-MYC R	GATCCAGACTCTGACCTTTTGC	
ERG F	CTCCTCCAGCGACTATGGA	57 bp
ERG R	GCGGCTGAGCTTATCGTAGT	
PTEN Exon7 F	GCTTGAGATCAAGATTGCAGATACAG	446 bp
PTEN Exon7 R	GTCTACCAATGCCAGAGTAAGCA	
TP53 F	GCGCCATGGCCATCTACA	511 bp
TP53 R	GTTGGGCAGTGCTCGCTTAGT	
RPS6 F	TTCAGCTGCTTCAAGATGAA	750 bp
RPS6 R	CTGACTGGATTCAGACTTAGAAGT	
TLX3/HOX11L2 F	GCGCATCGGCCACCCCTACCAGA	244 bp
TLX3/HOX11L2 R	CCGCTCCGCCTCCCGCTCCTC	
PICALM S1770	GCAATCTTGGCATCGGAAAT	440 bp / 380 bp
MLLT10 AS559	CGATCATGCGGAACAGACTG	
MLLT10 AS1002	GCGCTTCAATGATCCAGATATAGAG	

Viability of 8 primary T-ALL samples cultured for 72 hours in the presence or absence of IL7

UPN	PTEN <i>status</i>	% live cells			
		Before colture	72 h colture RPMI alone	72 h colture RPMI + IL7	Fold increase
21	wt	87	31.0	48.6	1,57
22	wt	93	43.2	44.2	1,02
23	wt	81	9.1	29.7	3,26
25	wt	92	38.2	40.2	1,05
5	mut	86	24.3	51.2	1.06
4	mut	93	47.3	15.2	1.09
20	mut	92	48.4	48.9	2.01
2	mut	86	13.9	49.1	1.04
Mean		88.8	31.9	40.9	1.51
median		89.5	34.6	46.4	1.08
range		(86-93)	(9.1-48.4)	(15.2-49.1)	(1.05-3.26)